

NUREG/IA-0055



# International Agreement Report

---

---

## An Assessment of TRAC-PF1/MOD1 Using Strathclyde 1/10 Scale Model Refill Tests

Prepared by  
W. M. Dempster, A. M. Bradford, T. M. S. Callander, H. C. Simpson

University of Strathclyde/Central Electricity Research Laboratories  
Kelvin Avenue  
Leatherhead, Surrey  
United Kingdom

Office of Nuclear Regulatory Research  
U.S. Nuclear Regulatory Commission  
Washington, DC 20555

March 1992

Prepared as part of  
The Agreement on Research Participation and Technical Exchange  
under the International Thermal-Hydraulic Code Assessment  
and Application Program (ICAP)

Published by  
U.S. Nuclear Regulatory Commission

## NOTICE

This report was prepared under an international cooperative agreement for the exchange of technical information.\* Neither the United States Government nor any agency thereof, or any of their employees, makes any warranty, expressed or implied, or assumes any legal liability or responsibility for any third party's use, or the results of such use, of any information, apparatus product or process disclosed in this report, or represents that its use by such third party would not infringe privately owned rights.

Available from

Superintendent of Documents  
U.S. Government Printing Office  
P.O. Box 37082  
Washington, D.C. 20013-7082

and

National Technical Information Service  
Springfield, VA 22161

NUREG/IA-0055



# International Agreement Report

---

---

## An Assessment of TRAC-PF1/MOD1 Using Strathclyde 1/10 Scale Model Refill Tests

Prepared by  
W. M. Dempster, A. M. Bradford, T. M. S. Callander, H. C. Simpson

University of Strathclyde/Central Electricity Research Laboratories  
Kelvin Avenue  
Leatherhead, Surrey  
United Kingdom

Office of Nuclear Regulatory Research  
U.S. Nuclear Regulatory Commission  
Washington, DC 20555

March 1992

Prepared as part of  
The Agreement on Research Participation and Technical Exchange  
under the International Thermal-Hydraulic Code Assessment  
and Application Program (ICAP)

Published by  
U.S. Nuclear Regulatory Commission

## NOTICE

This report is based on work performed under the sponsorship of the United Kingdom Atomic Energy Authority. The information in this report has been provided to the USNRC under the terms of the International Code Assessment and Application Program (ICAP) between the United States and the United Kingdom (Administrative Agreement - WH 36047 between the United States Nuclear Regulatory Commission and the United Kingdom Atomic Energy Authority Relating to Collaboration in the Field of Modelling of Loss of Coolant Accidents, February 1985). The United Kingdom has consented to the publication of this report as a USNRC document in order to allow the widest possible circulation among the reactor safety community. Neither the United States Government nor the United Kingdom or any agency thereof, or any of their employees, makes any warranty, expressed or implied, or assumes any legal liability of responsibility for any third party's use, or the results of such use, or any information, apparatus, product or process disclosed in this report, or represents that its use by such third party would not infringe privately owned rights.

## Summary

TRAC-PF1/MOD1 predictions of LOCA refill experiments carried out on a 1/10 scale model PWR vessel are presented. The predictions show that TRAC underpredicts bypass for the test cases considered. Comparison results are presented and discussed. Simple sensitivity analysis of the interfacial drag models used is presented in an effort to explain the poor performance of the code.



# CONTENTS

	<u>Page No.</u>
Summary	iii
Contents	v
Nomenclature	vii
1.0 Introduction	1
2.0 Experimental Test Facility	2
3.0 TRAC Nodalisation Scheme	5
4.0 Calculation Procedure	7
5.0 Results of TRAC Simulations	8
6.0 Discussion	12
7.0 Interfacial Drag Models	14
8.0 Conclusions	16
9.0 Further Comments	17
Acknowledgements	17
References	18
Appendix	
Table	
Figures	



## Nomenclature

A	Area ( $m^2$ )
$\alpha$	Void fraction
$C_d$	Drag coefficient
$C_i$	Interfacial drag coefficient ( $kg/m^4$ )
D	Diameter (m)
E	Entrainment fraction
g	Gravitation acceleration ( $m/s^2$ )
j	Superficial velocity (m/s)
$j^*$	Dimensionless superficial velocity
L	Length (m)
M	Mass flowrate (kg/s)
$\mu$	Viscosity ( $Ns/m^2$ )
Re	Reynolds number
$\rho$	Density ( $kg/m^3$ )
S	Circumference (m)
$\sigma$	Surface tension (N/m)
V	Velocity (m/s)
We	Weber number

## **Subscripts**

am	Annular mist
af	Annular film
d	Droplet
F	Full scale
g	Gas or vapour
h	Hydraulic
l	Liquid
m	Model
olf	Onset of entrainment
p	Pressure
r	Relative

## 1.0 INTRODUCTION

A continuous effort is being made to ensure that existing LWR safety codes, such as TRAC and RELAP are capable of predicting the behaviour of reactor safety related experiments and ultimately the behaviour of full scale nuclear plants. The performance of the codes used has given cause for concern in a number of areas e.g. their sensitivity to user experience, the numerical approximations made to solve the partial differential equations describing the system and the physical models used to describe the phenomenon occurring during accident conditions, such as a LOCA.

In a LOCA the main safety criteria is to maintain safe temperature levels in the fuel rods of the reactor core. This is achieved by scramming the reactor and endeavouring to replace the liquid mass lost through the break by introducing emergency core cooling water into the system and particularly into the reactor vessel. During a large break LOCA in a Pressurised Water Reactor (PWR), (double ended cold leg break) a particular critical phase of the transient may be reached when the emergency core cooling water is prevented from entering the vessel due to an opposing flow of steam originating from the core and intact loops. This phase of the transient, known as the Refill Phase, includes highly complex interactions of steam and water involving multi-dimensional, non-equilibrium counter-current two phase flows and attempts to predict such conditions employs thermal hydraulic codes, such as TRAC, to the limits of their capabilities.

The purpose of the work reported here is to focus attention on the capabilities of TRAC PF1/MOD1 (Ref. 1) to simulate the conditions existing in the vessel downcomer during the refill phase. Previous assessments of TRAC against separate effects downcomer experiments had already produced confusing results regarding TRAC's sensitivity to different nodalisations (Ref. 2). Also Coddington (Ref. 3) had identified the non-conservative formulation of TRAC's momentum equations as a possible source of problems. The physical models had also been identified as deficient by Cappiello (Ref. 4) who suggested that the interfacial film drag correlation for the annular mist regime underestimated the interfacial drag coefficient for the downcomer flows. This work has raised substantial doubt concerning TRAC's ability to model the refill phenomenon correctly and therefore the accuracy of the large plant calculations that had recently been carried out in the UK.

Turner (Ref. 5) is currently investigating the formulation problems associated with the mathematical modelling and has produced alternative formulations to overcome the non conservation of momentum produced by the numerical solution techniques. In conjunction with Turner's work the present exercise attempts to assess TRAC's capabilities against downcomer separate effects experiments carried out at Strathclyde University on a 1/10 scale model of a PWR vessel geometry (Ref. 6). The experiments established steady state refill conditions for various ECC and steam flowrates, liquid subcoolings and pressure effects. In addition to the above tests video films were made of the processes taking place within the downcomer. One of the main limitations of previous assessments of TRAC against downcomer separate effects is that comparisons were made against measurements of lower plenum liquid levels or mass flows into the lower plenum or out of the break without determining any of the details or conditions that exist in the downcomer. This then presents difficulties in assessing TRAC's flow regime map or corresponding models and correlations. With this in mind the present work sets out to compare a number of the Strathclyde experiments with TRAC predictions and to establish through the use of the video film recordings if TRAC is predicting similar flow features to that of the experiment. The version of TRAC PF1/MOD1 used in the exercise was the Winfrith modified code B05 and run on the Harwell CRAY 2 supercomputer.

## **2.0 EXPERIMENTAL WORK**

### **2.1 Test Facility**

The test facility was primarily designed to study the refill stage of a double ended cold leg break loss of coolant accident in a PWR; in particular cold leg injection of the emergency core cooling water.

The facility was designed for operation with steam/water and air/water as the working fluids and incorporated a closed loop recirculation system. Line diagrams of the flow loop are shown in Figs. 2.1 and 2.2. The reactor vessel test section was a 1/10 scale model of a Westinghouse Pressurised Water Reactor, with particular emphasis on the downcomer annulus. Two test sections were available, one with a transparent (polycarbonate) exterior, restricting operations to low pressure (up to 1.7 bar) and allowing visual observation; the other in stainless steel permitting higher pressure operation (up to 5.0 bar). A range of inlet water sub-coolings (inlet steam saturation temperature minus inlet water temperatures) was available ranging from 80 K down to almost zero.

The reactor vessel simulation included the provision of four hot legs (connected through the annulus to the core) and four cold legs (connected to the annulus only). Two of the hot legs were used to supply steam/air to the core; three of the cold legs were used as emergency coolant injection points, whilst the fourth represented the broken leg. Details and dimensions of the test section are shown in Fig. 2.3. The hot and cold leg connections were each 70 mm in diameter arranged circumferentially as shown in Fig. 2.4. This arrangement of hot and cold legs is typical of most PWR designs. However, the model downcomer incorporates a thermal shield facility which effectively separates the downcomer flow into two annular regions. This particular design of downcomer was associated with some Westinghouse and Combustion Engineering designs but is not included in the Sizewell PWR design.

The lower plenum had an outlet at the bottom (unlike the reactor system) so that the penetrating flow of the injected water could be measured in a calibrated tank. Adjustment of a valve in the lower plenum outlet pipe allowed a fixed level of water in the lower plenum to be maintained, therefore preventing the steam or air from leaving the vessel from the lower plenum.

## 2.2 Test Procedure

The main measurements taken during the tests included inlet steam/air flowrate, injected water flowrate, water penetrating to the lower plenum and various temperatures, pressures and pressure differences, as indicated in Fig. 2.2.

In the PWR refill studies, where the prime objective was to study the bypass phenomena, two particular types of test were involved, viz 'water first' and 'steam first' tests. In a water first test a particular water flowrate was set and then the steam flowrate increased to a specified value. This procedure was then repeated for increasing steam flowrates till complete bypass occurred.

In a 'steam first' test, for a particular steam flowrate the water flowrate was increased in steps until bypass ceased. The range of conditions tested during the study are indicated in Table 2.1.

## Steam/Water Tests

Mw	:	4680	-	26420 kg/hr
Ms	:	0	-	1700 kg/hr
$j^*_w$	:	0.015	-	0.083
$j^*_s$	:	0	-	0.194
$\Delta T_{sub}$	:	5	-	65 K

## Air/Water

Mw	:	5200	-	28360 kg/hr
Ma	:	0	-	1300 kg/hr
$j^*_w$	:	0.0159	-	0.0866
$j^*_a$	:	0	-	0.0805

Table 2.1 Range of Test Conditions

### 2.3 Video Observations

Separate from the above tests, visual observations were made and recorded by a video camera system for a range of conditions varying from total penetration to complete bypass for both steam/water and air/water situations. In the steam/water observations only the vessel outer casing was transparent, the rest of the section being stainless steel; thus only recordings of the events occurring in the annulus viewed below the broken leg were taken. In the air water tests, however the entire test section was transparent allowing observations to be made not only of the downcomer annular space but also of the cooling water inlet and its associated annular area and also of the broken leg outlet from the annular space.

The video films were not taken simultaneously with the actual experimental tests but were recorded prior to the experimental tests. For the steam/water situation twenty different conditions were filmed and for the air water case, eight conditions, all of which matched the experimental tests. The video recordings only observed the test section from particular directions, i.e. for the steam/water tests, only the conditions under the broken leg were recorded while for the air/water tests the regions under the broken leg and 90 degrees to the broken leg were recorded.

It should also be noted that the air/water visualisations were of a better visual quality than the steam/water since the air/water test section was constructed totally from transparent polycarbonate sections which gave good illumination of the downcomer. However, the steam/water tests incorporated a steel core liner which made illumination of the downcomer sections more difficult. Consequently, the quality of the steam/water videos are poorer making interpretation more difficult.

### 3.0 TRAC NODALISATION SCHEME

#### 3.1 Vessel Nodalisation

The nodalisation devised to simulate the 1/10 scale model refill experiments is shown on Figs. 3.1 and 3.2. The number of cells and their distribution are similar to the nodalisation schemes used in the TRAC large plant calculations that have recently been carried out in the UK (Ref. 7,8). Since the suitability of this nodalisation has not been proven for refill conditions it was thought reasonable to use this scheme as a starting point in any TRAC assessment. In addition it was decided to model the vessel geometry as accurately as possible with the inclusion of hot leg penetrations even though past work (Ref. 2) had produced conflicting results and raised many questions on the modelling of hot leg penetrations. Many of the questions that could undoubtedly be raised by this singular choice of nodalisation would be investigated at a later date after a better understanding of TRAC's capabilities had been gained from this first phase of computations.

The vessel nodalisation, shown on Fig. 3.2 includes 13 axial levels, 4 sectors and 1 radial ring to represent the downcomer, making eight regions in total. This is slightly different from the vessel nodalisation in the large plant schemes which consisted of an 11 x 4 x 3 grid. The core is modelled as in Fig. 3.2 and simply acts as a flow path for the steam or air. The lower plenum region has an additional level that was used to resolve various difficulties that were encountered during the initial debugging of the model. These problems were associated with the flow of steam from the core to the downcomer which had a tendency to reverse and flow back into the core when cooling water was injected into the downcomer. These problems were resolved by the inclusion of an extra level and by opening up the radial flow area in level 2. This flow area would not normally exist in practice due to the curvature of the lower plenum. However, this situation identifies one of the limitations of modelling spherical shapes using a coarse mesh cylindrical geometry. This departure from the true geometry is thought to have little effect on

modelling this experimental facility. It was also discovered that the downcomer was slightly longer when compared to a 1/10 linear scaling on the Sizewell PWR downcomer. Therefore an additional level was included in the downcomer region.

Referring to Fig. 3.1 the ECC injection flowrates were modelled using 3 FILL components, (1,2,3), injecting into 3 single cell PIPE components (11,12,13) corresponding to the 3 intact loop cold leg nozzles. The steam or air was injected into the core region using FILL component 4 and PIPE component 14, representing a hot leg nozzle. A BREAK component (5) was used to specify the experimental break pressure in the nozzle of the broken cold leg which was modelled using a PIPE component (15).

The liquid that penetrates the downcomer region exits the vessel through a drain pipe attached to the lower plenum. This was modelled by attaching a PIPE component (16) to the vessel and using the TRAC separator model (FRIC < -1.0E20, Ref.1) to ensure that steam did not leave the lower plenum with the liquid. A BREAK component (6) was connected to the pipe to specify an atmospheric boundary condition.

### 3.2 Heat Structure Modelling

The heat transfer from the downcomer walls can have a significant effect on the course of the refill process by increasing the ECC fluid temperature and limiting the effect of direct contact condensation. It was therefore important to try and model the heat transfer through the steel liner from the core steam to the downcomer fluid even though no experimental measurements were obtained for this heat transfer.

It is not possible to directly model the heat transfer between vessel hydrodynamic cells separated by solid structures using TRAC PF1/MOD1 therefore the one dimensional conduction slab model was adapted in an attempt to include downcomer wall heat transfer effects. The slab model used in the present study, is shown in Fig. 3.3 which shows a typical slab which could transfer heat to a downcomer hydrodynamic cell. The first node models the core steam temperature which remains at an approximately constant value throughout the test. However to maintain a constant temperature boundary condition at the first node an artificial material with a very high thermal capacity was input for this node. The thermal conductivity associated with this material corresponded to a value determined using the Dittus-Boelter convective heat transfer correlation.

### 3.3 Graphical Presentation

The huge amount of data that TRAC produces from simulations can be cumbersome to handle and therefore difficult to analyse without the aid of graphics post-processing tools. Therefore, several computer programs were written to analyse the fluid flow conditions predicted in the vessel downcomer. One program could produce the velocity or phasic mass flow vector distribution in the developed downcomer. In addition to the vector plots the representation of the liquid fraction was included for each cell. Fig. 3.4 indicates the developed downcomer solution grid with the corresponding cold leg junction points and hot leg blockage areas while Fig. 5.6 is a typical plot using the software. The hot and cold leg junction information was not included to improve clarity. It should be noted that the vector representing the liquid phase is always positioned on the left of centre in each cell while the vapour phase right of centre. Also the vectors are constructed using the same convention as used by TRAC i.e. each vector is constructed from the components of the positive cell face. For this exercise, positive cell faces in the axial direction are the higher cell faces and positive cell faces in the circumferential direction are the anti-clockwise face (right hand face).

The above software can produce a snapshot of the downcomer flows at any time in the calculation. To animate the process and therefore produce a motion picture of the transient further computer processing is required. The method used to do this at present is not very efficient but informative results can be obtained and displayed on a micro-computer if the effort is warranted.

### 4.0 CALCULATION PROCEDURE

Four tests (with corresponding video recordings) were chosen from the Strathclyde test data bank and covered the whole range of available conditions varying from total penetration to total bypass at moderately high subcooling and were thought to give the best possible assessment from the available data bank of video recorded tests. Table 4.1 shows the test conditions which were simulated with TRAC. The tests were renumbered A B C and D for ease of reference. TEST A was a steam/water total penetration test, TEST B and TEST C were partial penetration tests with steam/water and air/water respectively and TEST D was a high subcooling steam/water bypass test.

In addition to the above tests two further repeat calculations were carried out using a modified version of TRAC. These calculations were performed to take advantage of work being conducted by Turner (Ref. 5) who had attempted to overcome previously identified difficulties (Ref. 3) concerning the non-conservation formulation of the TRAC momentum equations. These further calculations repeated tests B and D and are identified as Tests B1 and D1.

Each TRAC calculation of an experimental test was performed in steam first mode. Steam was injected into the vessel core at the test flowrate and temperature until steady conditions existed (usually 5 secs). At this time the ECC water flowrate was ramped from zero to the test flowrate in each cold leg over 1 second and the calculation run for another 15 seconds.

## 5.0 RESULTS OF TRAC SIMULATIONS

### 5.1 Standard TRAC Calculations

#### Test A

Test A was a high subcooling total penetration test in which a high degree of thermal equilibrium was reached, i.e. the maximum amount of steam was condensed for the available liquid flow and subcooling. The TRAC prediction of this test is shown in Figs. 5.1 and 5.2 and indicates that TRAC calculated the correct situation with all the injected liquid flowing to the lower plenum. However TRAC slightly under predicted the amount of steam condensed in the vessel which was calculated to be almost 57% of the inlet steam flow while 66% of the steam flow was measured to be condensed in the experimental tests. Fig. 5.3 indicates the vector and liquid fraction distribution during the calculation. Counter-current flow is observed in all cells in the downcomer with liquid flowing into the lower plenum from regions 6, 7 and 8. The video recordings of this situation show calm conditions in the downcomer with indications that the liquid is distributed all around the downcomer by the time it reaches the lower plenum. Overall TRAC predictions agree well with the experimental results.

#### Test B

Test B was a partial penetration test with approximately 45% of the inlet water flow bypassing the lower plenum and the other 55% reaching the lower plenum. The TRAC comparison with

the experimental results can be seen in Figs. 5.4 and 5.5 and show a far greater amount of liquid predicted to penetrate the downcomer than in the test and subsequently a lower amount of liquid bypassing the downcomer. Steady conditions were reached fairly rapidly during the calculation.

Figs. 5.6 and 5.7 are vector plots of the phase velocities and mass flows and also include the liquid fraction distributions in each cell at 19 secs into the calculation. These two figures show clearly the source of the lower plenum and bypass liquid flowrates. The majority of the liquid bypassing the downcomer originates from the cold leg attached at region 6, though a small amount does flow from region 8. This is not surprising since there is no hot leg blockage between region 5 and 6 which will reduce the circumferential flowrate between regions, at this level. The liquid flowrate injected into region 7 (farthest from the break) flows axially downwards, however the remaining unbypassed liquid injected into region 6 flows downwards redistributing into region 5 to mix with circumferential flow from region 8 to flow uniformly into the lower plenum.

The steam flows counter-current to the liquid flow in the majority of the downcomer cells and requires to circulate the hot legs to reach the cell attached to the broken leg as seen in Fig. 5.6. During the tests almost 30% of the steam flow was condensed in the vessel which closely corresponds to the maximum obtainable for thermal equilibrium conditions, however this was under-predicted by TRAC since approximately 20% of the steam was condensed in the vessel.

The video film, which only shows the situation in region 5 indicates partial penetration but with intermittent liquid sweep - out of the lower plenum. The liquid penetrating the downcomer seems to come from regions opposite the break some of which will be dragged back into the downcomer. Liquid is believed to exist in region 5 and is thought to originate from circumferential flow from regions 6 and 7 however, there are no indications that this liquid reaches the lower plenum and is believed to flow co-currently with the steam out of the break. Thus there is poor agreement between TRAC predictions and the experimental measurements and the observed flow patterns in the downcomer.

## Test C

Test C was an air/water partial penetration test where 75% of the inlet liquid flowrate is bypassed across the downcomer and out of the break. Figs. 5.8 and 5.9 compare the experimental break

and lower plenum mass flowrates with that calculated by TRAC. The results are in very poor agreement with the experimental values with the majority of the inlet liquid flow being calculated by TRAC to penetrate the lower plenum, i.e. a total penetration situation.

The velocity vector and liquid fraction distribution are shown on Fig. 5.10 which shows counter-current flow in most of the downcomer cells. The liquid flowrate entering regions 6 and 8 is distributed circumferentially to produce a uniform flowrate into the lower plenum. It was interesting to note that very high liquid velocities were predicted (approximately 3 - 5 m/s) and were comparable with the vapour velocities.

The video film in this case is clearer than in the steam-water tests with the advantage that the film was taken at two positions, 90 degrees to each other covering regions 5 and 8. The indications here are that partial penetration takes place particularly in regions 6, 7 and 8 where counter-current flow is observed. In region 5 however it would appear that the water is carried upwards into the downcomer by the air but moves circumferentially and joins a disturbed region with liquid flowing downwards in the adjacent regions leaving a clear passage for the air to ascend. In the upper region of the downcomer, at the cold leg positions both the liquid and the air move circumferentially around the downcomer.

From the second observation position covering region 8 it is noted that

- (1) most of the penetration to the lower plenum comes from the cold leg injection points diametrically opposite the break, while the majority leaving the break originates from the cold leg nearest the break.
- (2) the least resistance to the passage of air is in region 5, where no falling liquid is evident.
- (3) in region 8 there is a transition region, between complete penetration and total bypass in which the flow is highly chaotic and appears unstable, similar to churn flow in pipes.
- (4) in the downcomer at the break level the flow appears almost completely circumferential for both phases and moving towards the break, flowing above and below the hot leg blockages.

As is apparent these conditions are not predicted by TRAC at any point in the downcomer.

#### Test D

Test D was the most rigorous assessment of TRAC performed during this phase of tests, consisting of a total bypass condition at a relatively high subcooling of 37 K.

The cold leg break and lower plenum mass flowrates both measured and calculated are shown on Fig. 5.11 and Fig. 5.12. TRAC predicted that the majority of the liquid flowing into the downcomer was held up and bypassed the downcomer in a fluctuating manner during the first 7 seconds of cooling water injection. The velocity, liquid fraction and phasic mass flow vector distribution at 19.6 seconds are shown on Figs. 5.13 and 5.14 respectively. These figures show that by this time the majority of the liquid penetrating the downcomer did so via region 7, the region farthest from the break with no liquid existing in the other downcomer regions. The sequence of events over the first 5 seconds of the transient calculation showed that all of the injected water was held up in the upper downcomer which led to the high bypass rates shown in Fig. 5.11. The injected liquid in regions 6 and 8 travelled upwards and around the upper downcomer levels (12 and 13) towards region 7. The liquid then flowed downwards into the lower plenum.

TRAC calculated that approximately 55% of the steam flow condensed in the downcomer which compared well with the measured value of nearly 57% of the steam flow condensed in the vessel. The video film however, indicates that very little water reaches and remains in the lower plenum. Intermittently some liquid may penetrate the downcomer from the opposite side of the downcomer to the break but will be pulled back into the downcomer region which becomes a very chaotic turbulent mixture of steam and water.

## 5.2 Modified TRAC Calculations

Two of the above calculations were repeated with a modified version of the TRAC code in which the momentum equations were set in conservative form, (Ref. 5). These were Test B1 and Test D1 in Table 4.1. Fig. 5.15 indicates a comparison between the break mass flows for calculations B and B1 and show very little improvement in the overall prediction. However, noticeable differences between the calculations are seen when comparing the overall distribution of liquid fractions and velocities, Fig. 5.16. This figure indicates an increase in the liquid fractions in

most cells and a greater concentration in region 5 when compared with Fig. 5.10. The most dramatic difference was found to occur when recalculating the total bypass test (Test D1). It was now found that TRAC correctly predicted total bypass as is shown in Fig. 5.17 which shows an unsteady break mass flow. The liquid fraction and phase velocity distributions, Fig. 5.18 and phasic vector mass flows, Fig. 5.19 indicate liquid hold up in the upper sections of the downcomer. It is also interesting to note that some liquid would intermittently penetrate the downcomer but be swept back up and out the break as was observed using a computer generated movie of the transient sequence.

## 6.0 DISCUSSION

### 6.1 Downcomer Flow Patterns

Some general points can be made from the video films regarding counter-current flow in the downcomer even though the video recordings were somewhat limited. The asymmetric nature of the break and injection points leads to an asymmetric two dimensional flow pattern which can be described by discussing conditions ranging from partial to total penetration. At partial penetration all of the liquid entering from the two cold legs farthest away from the break, flows down into the downcomer below the hot legs and is distributed circumferentially around the downcomer to meet a churn turbulent region, Fig. 6.1. In this region the liquid tends to be directed upwards and out of the break. However, liquid does tend to flow into the lower plenum from the region below the injection points. The liquid entering from the cold leg nearest the break partially flows circumferentially towards the break or drops down into the downcomer. However this liquid flow enters into the turbulent mixing region where it may then be entrained and flow towards the break. The extent and effect of the mixing region is dependent on the amount of steam or air flowing in this section and therefore can be reasoned to extend around the downcomer during greater bypass conditions.

One point to note is that there is sufficient circumferential distribution of conditions in the downcomer to warrant a greater number of segments in the TRAC nodalisation scheme than used in the present simulation. However an increase in the number of cells may not necessarily improve the predictions if the TRAC interfacial models are inappropriate for the conditions that exist in the downcomer. Also the various forms of averaging that occur in the 3-dimensional closure models may have a significant effect on the calculation procedure. For example, the void

fraction in each cell not only determines the flow regime but is used to determine interfacial drag coefficients. However the actual void fraction used in the equations is an averaged value based on neighbouring cell void fractions and weighted by using the cell lengths i.e.

$$\alpha = (L1 * \alpha1 + L2 * \alpha2)/(L1 + L2)$$

This implies that the interfacial models are coupled to the cell dimensions and therefore the degree of nodalisation used in the calculation. This could contribute to the sensitivity of the calculation to the hot leg blockage modelling as reported by Slovik (Ref. 2).

## 6.2 Summary of Results

The comparison of results obtained using the standard TRAC with those from the experiments show that the code consistently under-predicts the amount of bypass. This, in addition to the under prediction of the amount of steam being condensed suggest that deficiencies in the interfacial drag modelling exist. This conclusion has also been reached by Cappiello (Ref. 4) whose studies suggest that the Wallis interfacial friction factor used in TRAC to model the annular film interfacial friction factor should be multiplied by 5 to improve the overall prediction of bypass.

It is apparent, from the additional calculations (section 5.2) that using the modified code, with a conservative formulation of the TRAC momentum equations, can produce results which are substantially different from those obtained using the original non-conservative formulation. Since the modified TRAC produces better predictions and is a more correct formulation, the conservative formulation of the momentum equations should be used together with suitable experimental data to determine the validity of the interfacial closure relations.

Both the interfacial heat transfer and friction models require further investigation. However since TRAC did not adequately predict the appropriate flow conditions in the downcomer it is unlikely that a proper assessment of the interfacial heat transfer models can be made at this point, though it is interesting that the predicted condensation rates were of a similar order to the measured rates when the flow regimes were not. It should also be noted that the steam temperature used as a boundary condition for the downcomer wall heat transfer was found to be several degrees too high which resulted in an overestimate of the heat transfer to the downcomer fluid and is a contributing factor for the low steam condensation rates.

In the following section an exercise has been carried out to investigate the range of applicability of the correlations used to model the TRAC annular mist flow regime since it is believed that the interfacial drag is dominant in determining the flow regimes.

## 7.0 TRAC ANNULAR-MIST INTERFACIAL DRAG MODELLING

### 7.1 Interfacial Drag Coefficients

In TRAC the annular mist flow regime covers the void fraction range from 0.75 to 1.0. This regime is particularly important during the refill period since the void fractions in the downcomer are believed to fall within this range. However, it could be argued that void fractions less than 0.75 might occur during total bypass. TRAC would then calculate the interfacial drag coefficients from the slug/churn regime models but this will not be investigated in this report. The correlations that are used to calculate the interfacial drag coefficients are outlined in Fig. 7.1 (from Ref. 9) and show that the interfacial drag coefficient is calculated from the weighted summation of an annular film drag coefficient, based on a correlation by Wallis, (Ref. 10) and a droplet drag coefficient (Ref. 9). The entrainment fraction  $E$ , calculated using the maximum of two correlations determined by Kataoka and Ishi or Liles, is used as the weighting parameter to determine the total drag coefficient for the annular mist regime. The droplet diameter of the liquid existing in the mist flow is calculated using a constant Weber number of 4.0.

A small computer program was written at Strathclyde to carry out sensitivity calculations on the annular mist models. The program has been created using the information obtainable from the TRAC Models and Correlations document, (Ref. 9) and conforms to the Fortran coding in the TRAC subroutine TF3DE which contains the interfacial relationships for the 3-dimensional flow equations. The object of the exercise was to determine how each of the terms in Equation (1) (Fig. 7.1) related to each other for the typical conditions that existed during the previously discussed calculations. Therefore the geometry used during the sensitivity calculations related to the 1/10 scale model and fluid properties were for saturated conditions at 1 bar. Also the vapour velocities calculated by TRAC (Section 6.0) determined the range of the sensitivity studies and covered velocities from 0 to 30 m/s.

Fig. 7.2 shows the variation of the film, mist and combined drag coefficients with void fraction for various velocities. The results show that for these conditions the mist drag coefficient is

many magnitudes larger than the annular film drag coefficient across the whole void fraction range.

The consequence of this is that the entrainment fraction plays an important role in determining if the annular film coefficient has any significance in the total drag coefficient. Fig. 7.3 shows the variation of the entrainment fraction with velocity for an arbitrary void fraction of 0.85. This indicates that up to 10 m/s the entrainment is negligible and the interfacial drag coefficient is dominated by the annular film drag coefficient and from 10 m/s onwards the increasing entrainment causes the total drag to be quickly dominated by the droplet drag.

The above arguments when applied to the present steam/water calculations on the 1/10 scale model showed that only the predictions for TEST A produced velocities lower than 10 m/s in the downcomer annulus. Therefore any deficiencies in the modelling could be attributed to the Wallis correlation. This is in contrast to the TEST B and D predictions, where velocities were greater than 10 m/s and which were therefore dominated by the interfacial drag coefficient for the droplet. Cappiello (Ref. 4) has already suggested and used in TRAC an alternative correlation by Bharathan (Ref. 11) which is more appropriate to counter-current flow than the Wallis correlation (applicable only to co-current flow in tubes) and found it to produce better results. This was attributed to the fact that this correlation produces interfacial film drag coefficients which are approximately 5 times higher than those predicted by the Wallis correlation for the 1/5 scale Creare conditions. A similar exercise carried out using the geometry of the full scale plant is now discussed.

One of the main contributions to the uncertainty in two phase flow calculations is the validity of the physical models for different scaled geometries. With this in mind, the previous sensitivity calculations were repeated for conditions which are thought to exist during the refill phase in a full scale downcomer. It should be noted that the magnitude of the steam velocity in the full scale facility during the injection period would be approximately 1 to 3 times larger than in the 1/10 scale model if  $j^*$  for steam flow could be used as a scaling criterion (see appendix 1).

Fig. 7.4 shows the calculation for a pressure of 5 bar and Fig. 7.5 for a pressure of 20 bar. Both of these figures show that substantial entrainment occurs at very low velocities and therefore the total drag is completely dominated by the significantly high droplet drag (both curves lie on top of each other). This implies that the liquid would be totally dispersed in the vapour flow which is unlikely to be the case since total and partial penetration refill conditions are likely to exist for these low vapour velocity conditions and the liquid therefore exists as a falling film type flow.

However this may be one reason why TRAC has been found to correctly predict bypass since very high drag coefficients exist in mist flows and would be sufficient to force the liquid to flow upwards.

There is one important point worth noting concerning the relatively high droplet drag coefficients in Fig. 7.3. For counter-current flow conditions TRAC is likely to overpredict the droplet drag. The reason for this can be seen in Equation (4) Fig. 7.1 where the mist coefficient is dependent on the reciprocal of the droplet diameter. The constant Weber number criterion used to determine the droplet diameter may substantially underpredict the droplet diameter since the relative velocity is based on counter-current flows and not on the entrained droplet velocity which is likely to be close to the vapour velocity.

Therefore from the above discussion it is clear that a more detailed examination of the annular mist interfacial friction models is required. This would include establishing more appropriate annular film, droplet drag and entrainment models for counter-current flow conditions.

## 8.0 CONCLUSIONS

1. The Strathclyde videos have shown that the refill process is highly complex involving various flow regimes distributed around the downcomer, (e.g. Fig. 6.1). The spatial distribution of flow regimes is such that the current quadrant type vessel nodalisation is believed to be insufficient to capture the 2-dimensional effects of the process.
2. TRAC has been found to under-predict the amount of bypass as measured in the Strathclyde 1/10 scale PWR model refill experiments studied.
3. An analysis of the current interfacial drag modelling in TRAC has shown that the film and droplet drag coefficients and the entrainment correlations are unlikely to be appropriate for the conditions that exist in the vessel downcomer at any scale.
4. The use of the conservative form of the momentum equations in the code can, for the cases studied, produce better results than the standard code and therefore any future calculations should be carried out using the momentum equations set in the conservative form.

## 9.0 FURTHER COMMENTS

Phase II of the present contract will cover nodalisation sensitivity studies. It is hoped that varying the solution grid dimensions will identify TRAC's sensitivity to the nodalisation and explain the results obtained by Slovik (Ref. 2). This work will also attempt to explain the effect of nodalisation on the property averaging procedures used in the code (section 6.1).

Alternative correlations, more applicable to the counter-current flow conditions existing in the downcomer must be sought. It has already been shown (Ref. 4) that the existing interfacial film drag correlation under-estimates this effect. Other interfacial effects e.g. entrainment, heat transfer etc. should be similarly investigated.

Early in this study it was realised that the quality of the available video recordings of the downcomer flow conditions were inadequate to properly understand the physical processes occurring during the tests. A rebuild of the test rig has therefore been undertaken to make more detailed studies of the flow regimes existing during the counter-current flow conditions of the refill process.

### Acknowledgements

The work described in this report was sponsored by the Central Electricity Generating Board. However the comments and conclusions contained within this report are those of the authors and may not represent the opinions of the sponsors.

## REFERENCES

- (1) Liles, D.R. et al TRAC-PF1/MOD1: An Advanced Best-Estimate Computer Program For Pressurised Water Reactor Thermal Analysis, (NUREG/CR-3858). July 1986.
- (2) Slovik, G.C., Saha, P. Independent assessment of TRAC-PF1/MOD1 code with BCL ECC Bypass Test, 1985, NUREG/CR-4252.
- (3) Coddington, P. Private communication, 1987.
- (4) Cappiello, M. Assessment of the annular mist interfacial shear in TRAC-PF1/MOD1 against downcomer bypass and tie-plate flooding data, 1985 ASME 84-WA/HT-84.
- (5) Turner, D. A study of some discretisation effects in TRAC-PF1/MOD1 on the predictions of low subcooling counter-current flow, 1988 PWR/HTWG/P(88)592.
- (6) Rooney, D.H. et al Steam Water Flooding or Bypass in PWR Downcomer Annuli, 1985, European Two Phase Flow Group Meeting, Southampton.
- (7) Evans, F. Analysis of a Double Ended Cold Leg Break Loss of Coolant Accident for a Four Loop PWR using TRAC-PF1/MOD1 TUG/P(87)23, January 1987.
- (8) Dempster, W. The Simulation of a Double Ended Cold Leg Break with the Simultaneous Rupture of 16 Steam Generator Tubes using the TRAC-PF1/MOD1 Computer Code TUG/P(88) 90, August 1988.

- (9) Liles, D.R. et al                    TRAC-PF1/MOD1 Models and Correlations, 1988  
PWR/LCVSG/A(88).
- (10) Wallis, G.                            One Dimensional Two Phase Flow, McGraw Hill, 1969.
- (11) Bharathan, D.                        Air-Water Counter-current Annular Flow, EPRI NP-1165,  
September 1979.



APPENDIX. 1

$$j^* = \frac{M_g}{\rho_g A} \cdot \left( \frac{e_g}{g S (e_f - e_g)} \right)^{\frac{1}{2}}$$

For full scale to model scaling of bypass, assume  $j_F^* = j_M^*$

also set  $\frac{M_g}{\rho_g A} = V_g$  and  $(e_f - e_g)_F \approx (e_f - e_g)_M$

then  $V_{gF} \times \left( \frac{e_g}{S} \right)_F^{\frac{1}{2}} = V_{gM} \times \left( \frac{e_g}{S} \right)_M^{\frac{1}{2}}$

$$\therefore \frac{V_{gF}}{V_{gM}} = \sqrt{\frac{e_{gM}}{e_{gF}}} \times \sqrt{\frac{S_F}{S_M}}$$

for  $\frac{1}{10}$ - scale model,  $S_F = 10 S_M$

$$\frac{V_{gF}}{V_{gM}} = \sqrt{\frac{e_{gM}}{e_{gF}}} \times \sqrt{10}$$

for  $p = 1 \rightarrow 20$  bar,  $\frac{e_p}{e_{p=1}} = 1 \rightarrow 16.7$

hence  $\frac{V_{gF}}{V_{gM}} = 3.1 \rightarrow 0.79$

---

TEST	EXP. ID	FLUID	$M_w$ (kg/s)	$M_v/M_s$ (kg/s)	$M_{v,p}$ (kg/s)	$\Delta T$ (K)	$J^*_w$	$J^*_v$	$J^*_{v,p}$	TYPE	TRAC VERSION
A	25038012	STEAM/WATER	1.451	0.145	1.575	35.0	0.0162	0.0675	0.018	TOTAL PEN.	STANDARD B05
B	01048023	STEAM/WATER	2.516	0.214	1.372	12.6	0.0286	0.0918	0.0158	PARTIAL PEN.	STANDARD B05
B1	01048023	"	"	"	"	"	"	"	"	"	TURNERS
C	15068168	AIR/WATER	7.65	0.266	1.984	0.0	0.0841	0.0589	0.0218	PARTIAL PEN.	STANDARD B05
D	26838046	STEAM/WATER	4.888	0.403	0.0	37.6	0.0549	0.1625	0.0	BYPASS	STANDARD B05
D1	26838046	"	"	"	"	"	"	"	"	"	TURNERS

TABLE 4.1 TEST CONDITIONS

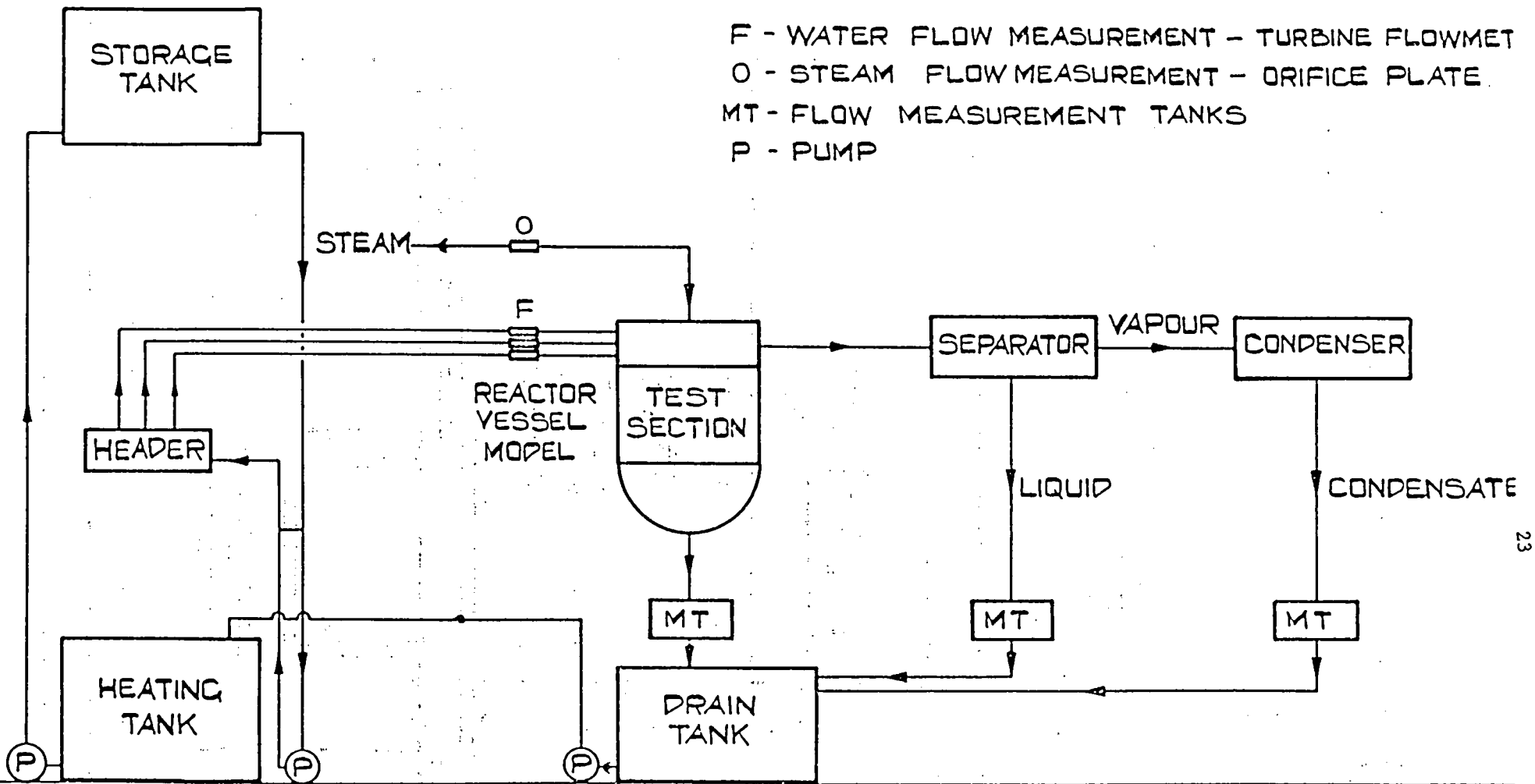


FIG.2.1 LINE DIAGRAM OF NEW P.W.R. REFILL TEST RIG

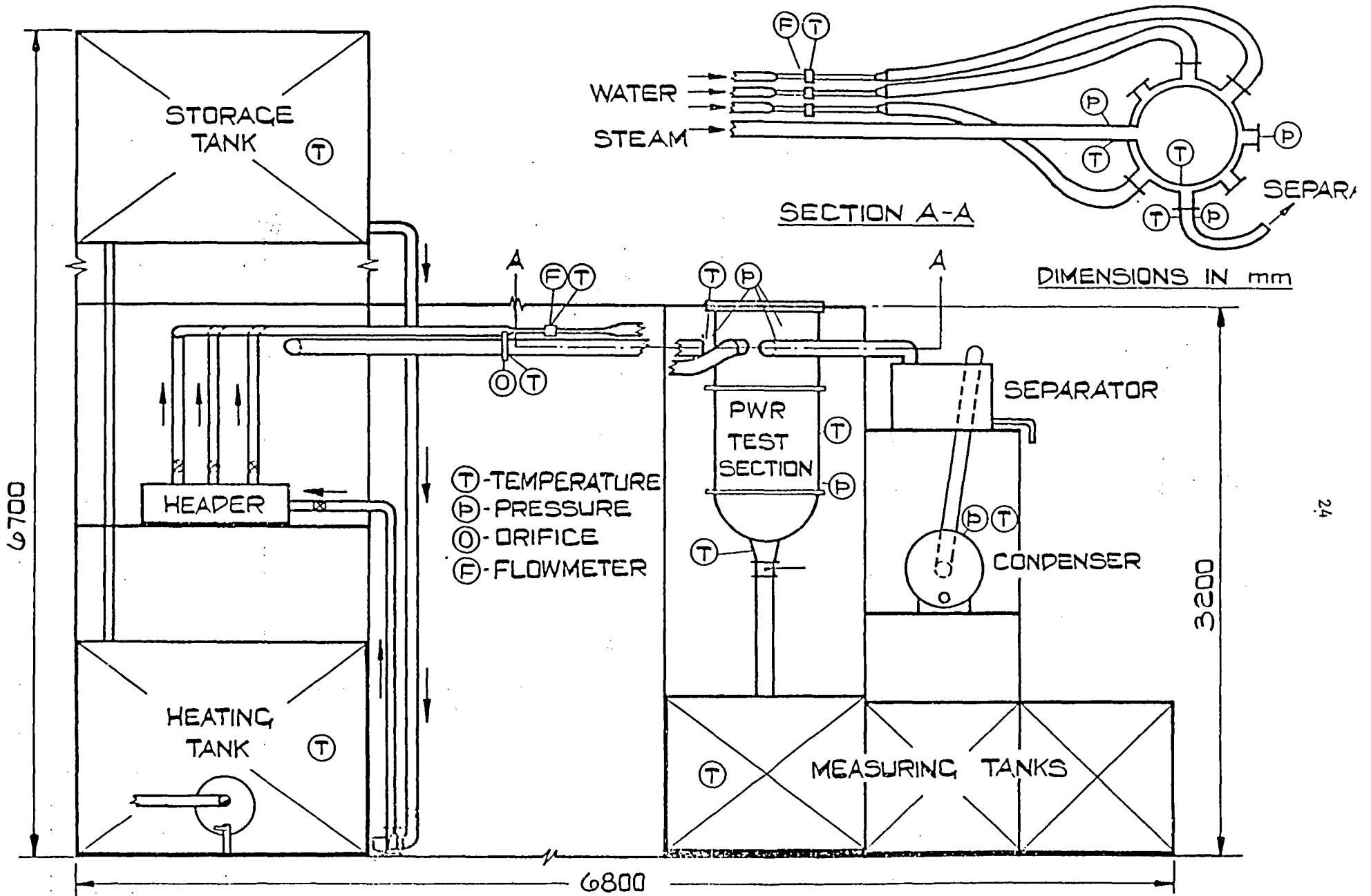


FIG. 2.2 LAYOUT OF NEW P.W.R TEST RIG

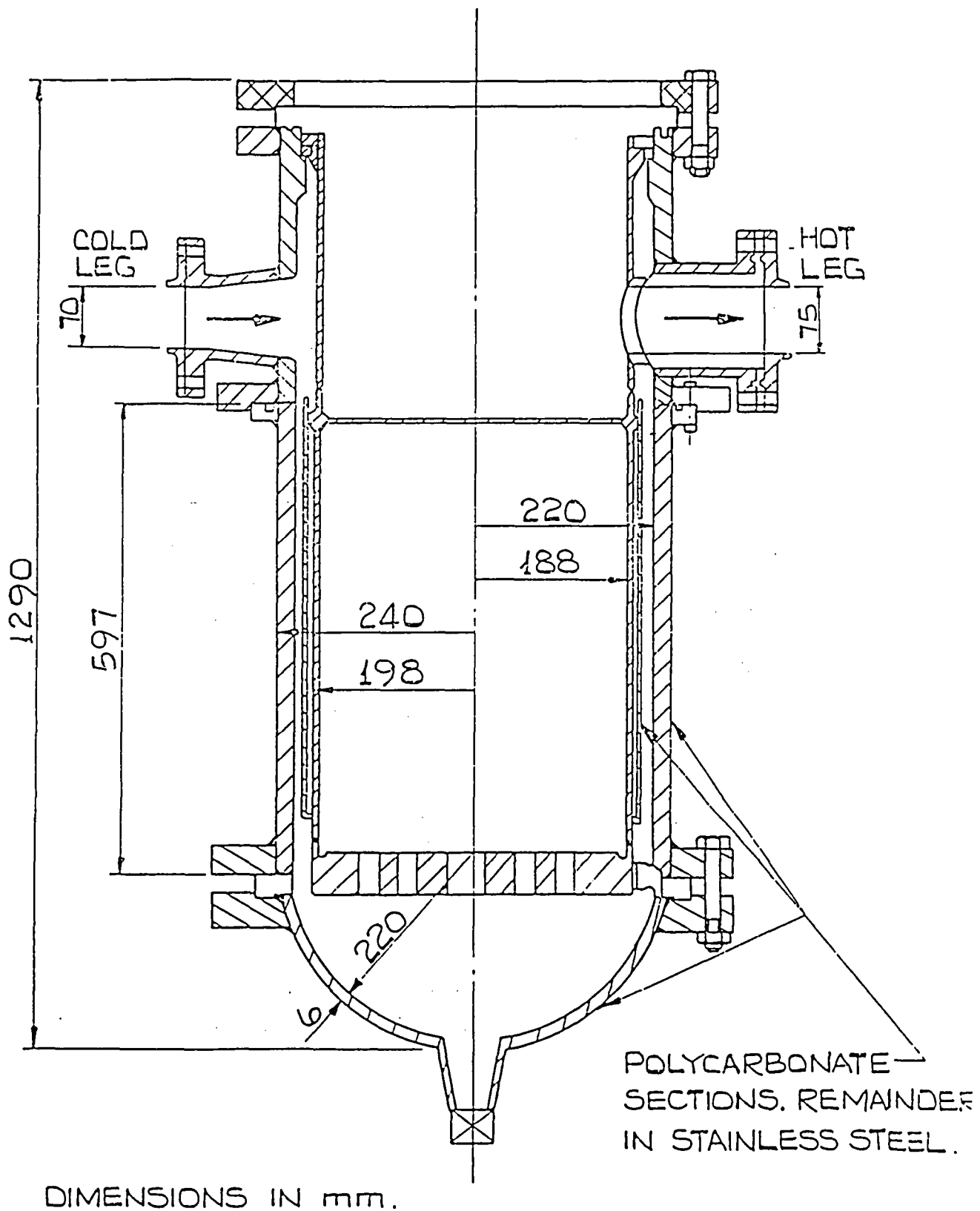


FIG. 2.3.      DETAILS OF TEST SECTION.

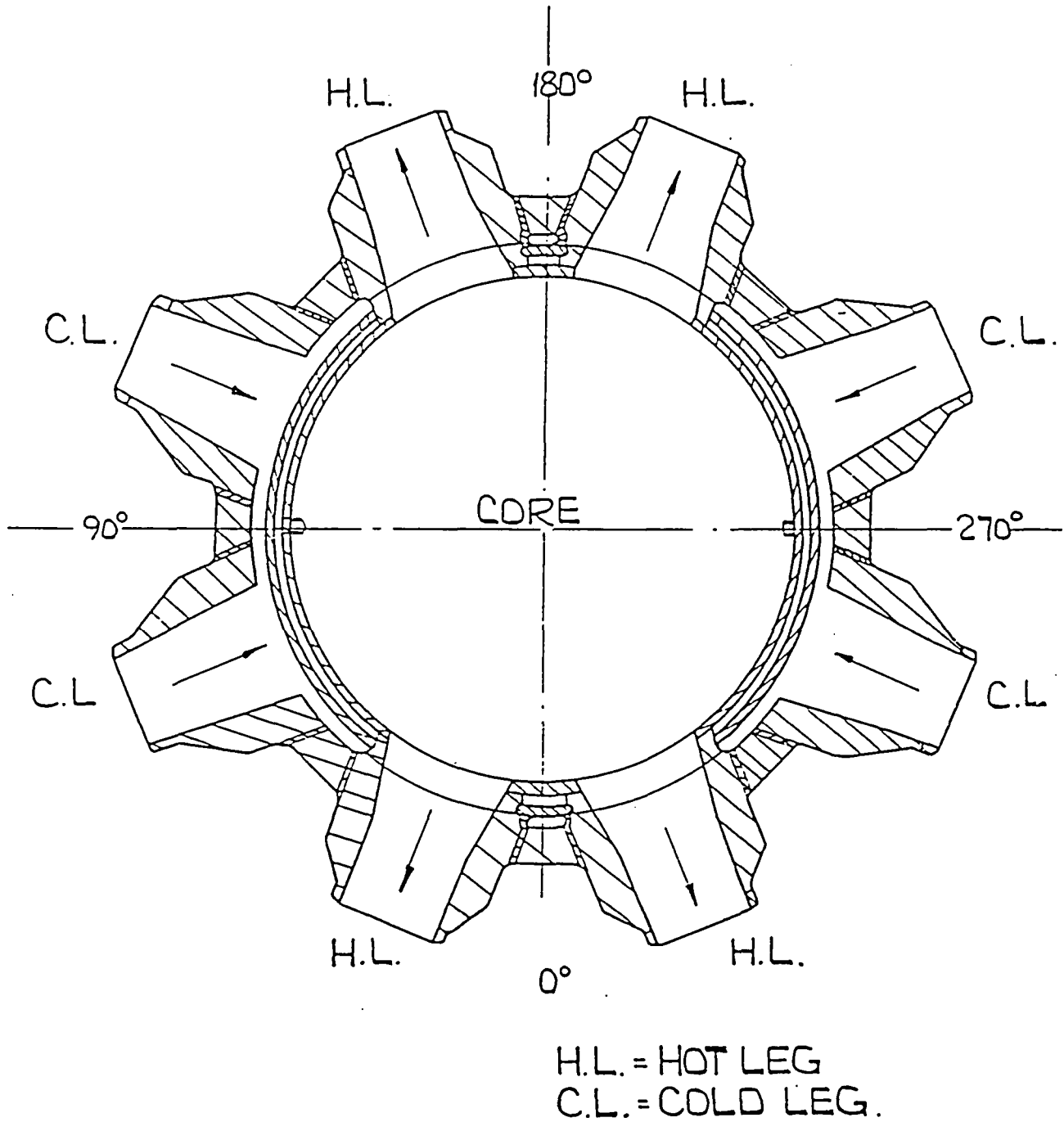


FIG.24.      CIRCUMFERENTIAL ARRANGEMENT OF  
HOT AND COLD LEG CONNECTIONS.

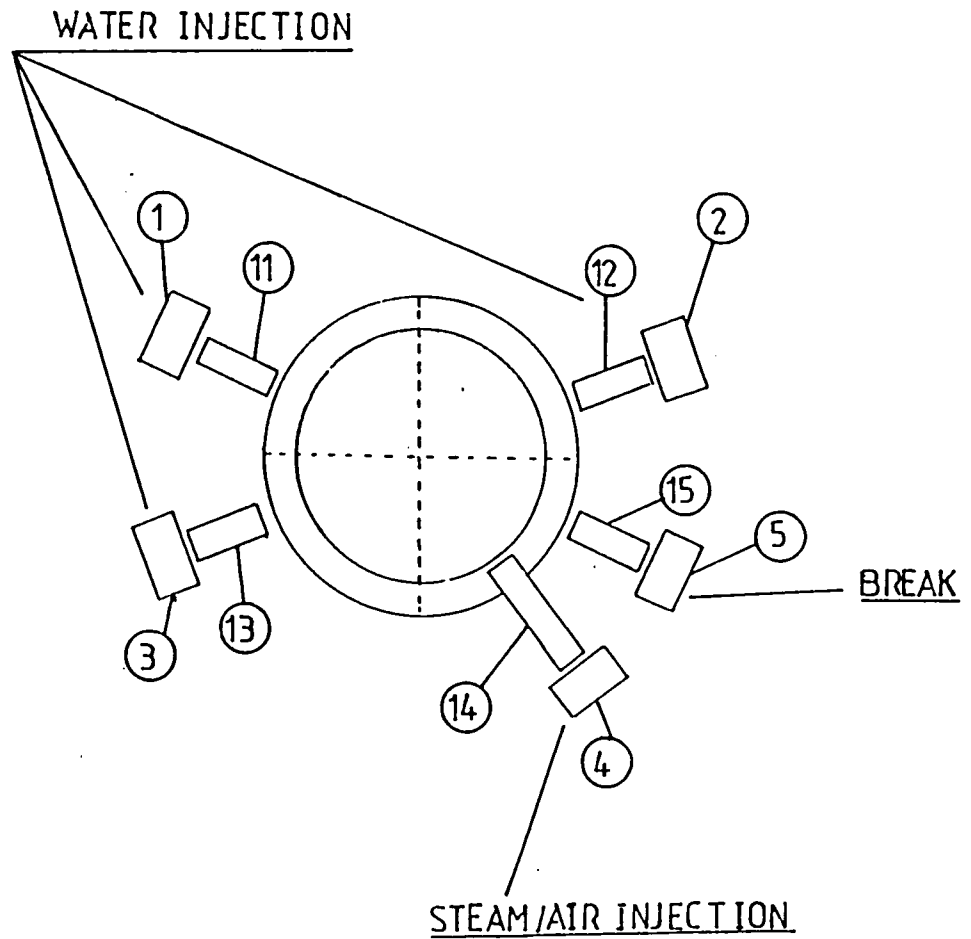
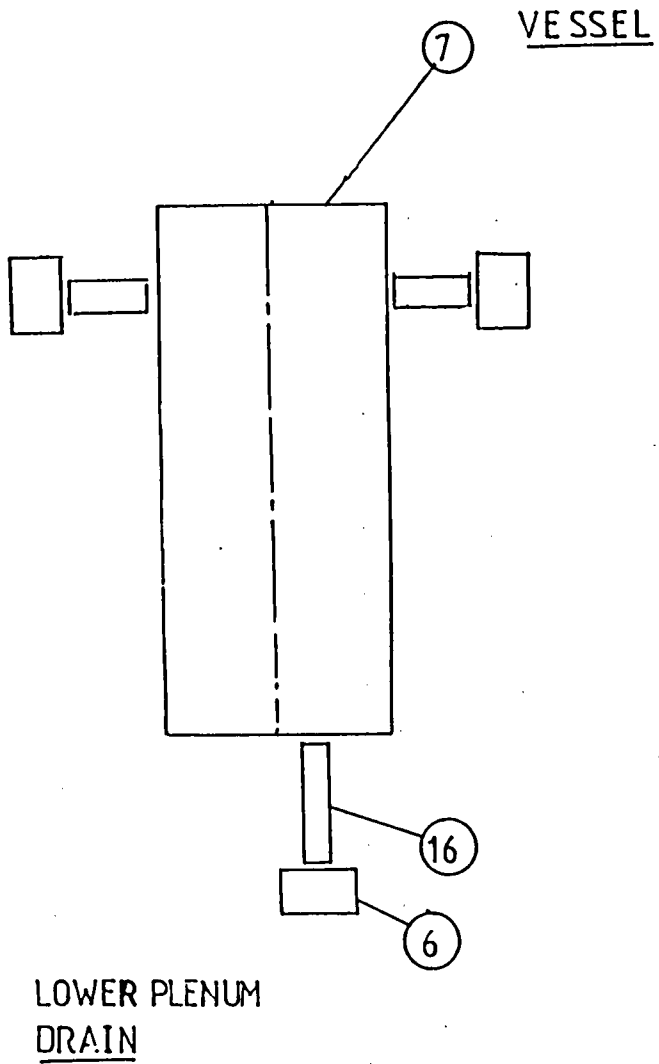
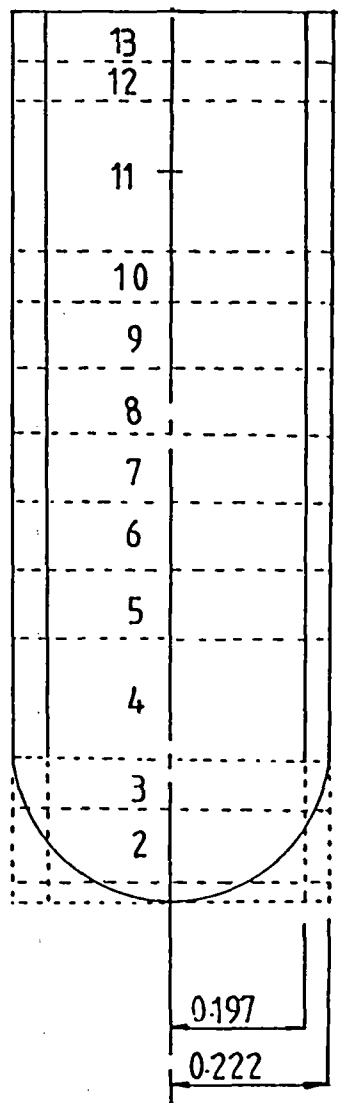
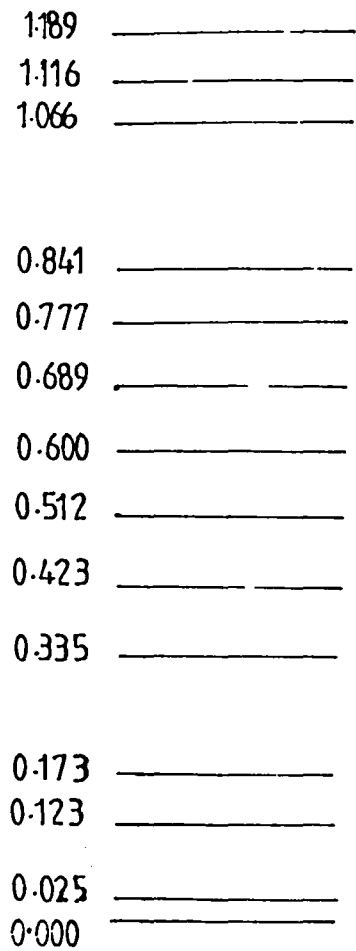


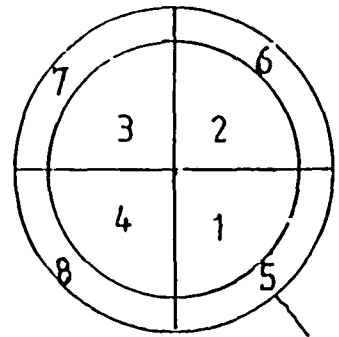
FIG. 3.1 NODALISATION SCHEME FOR REFILL RIG

Elevation



Hot and cold leg connections

Bottom of Downcomer



BREAK

FIG. 3.2 DETAILS OF VESSEL NODALISATION

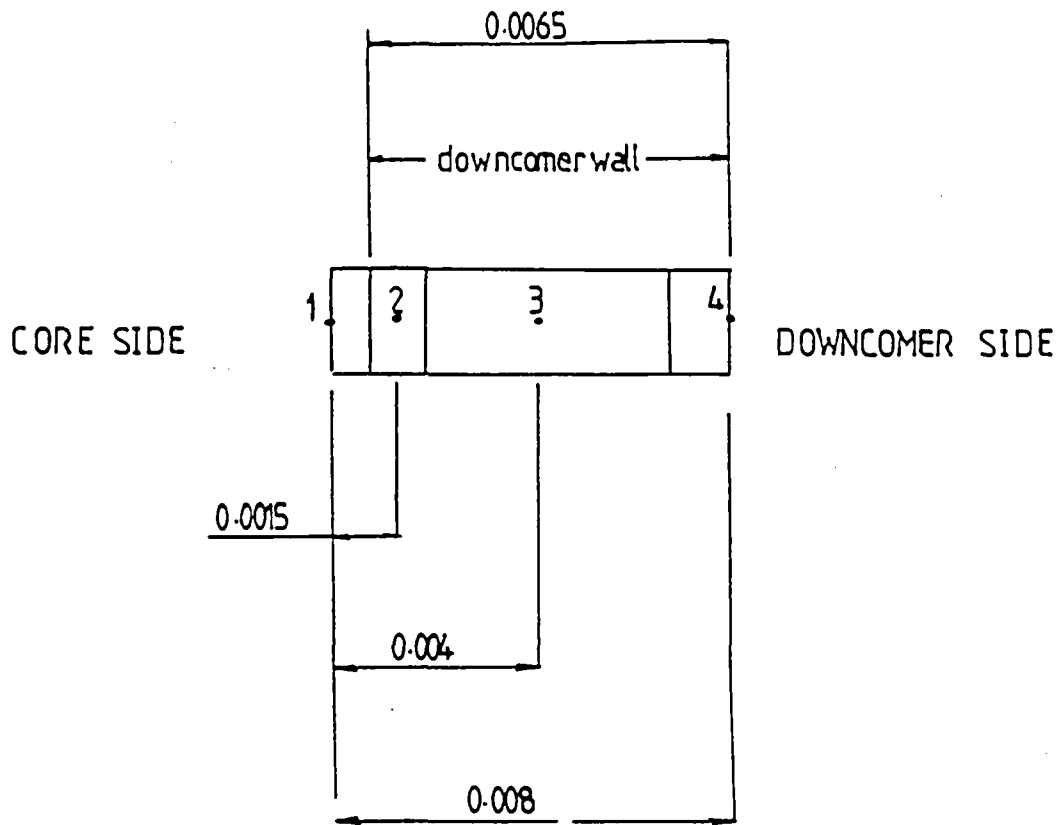


FIG. 3.3 NODALISATION OF DOWNCOMER WALL



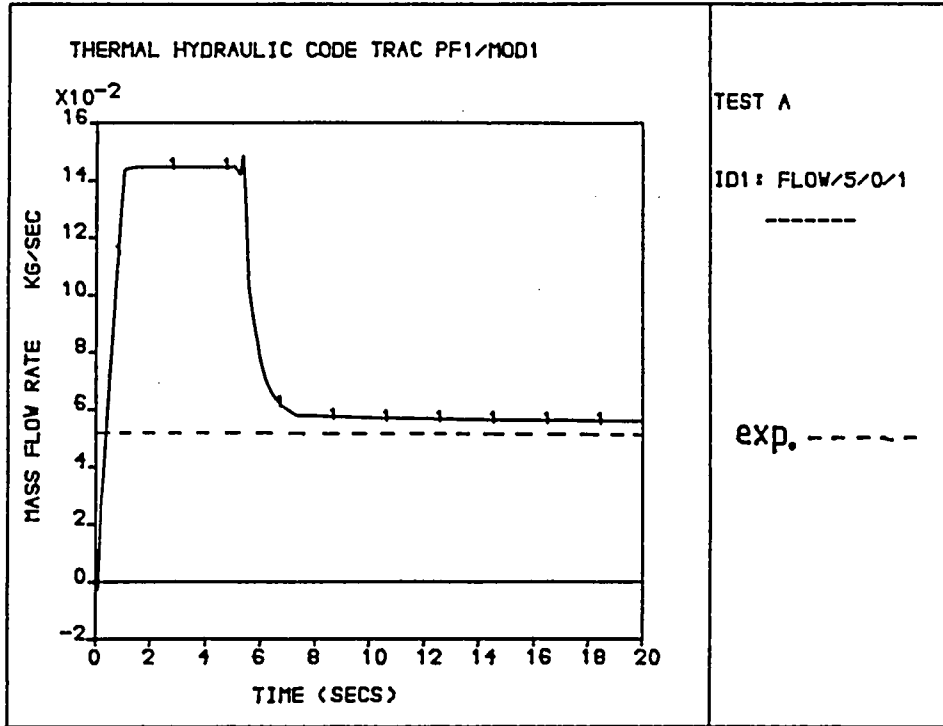


FIG. 5.1 TEST A ; EXPERIMENTAL AND PREDICTED BREAK MASS FLOWRATES

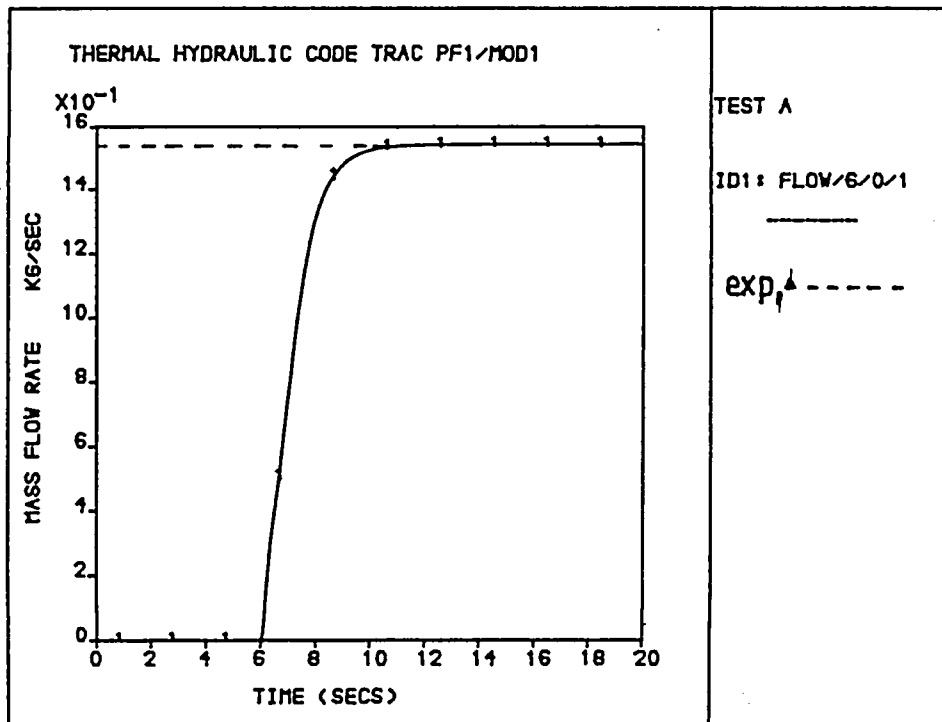


FIG. 5.2 TEST A ; EXPERIMENTAL AND PREDICTED MASS FLOWRATES FROM LOWER PLENUM

FILE : TEST A

TIME 19.04 secs

→ vap. vec.  
⇩ liq. vec.  
⊗ liq. frac.

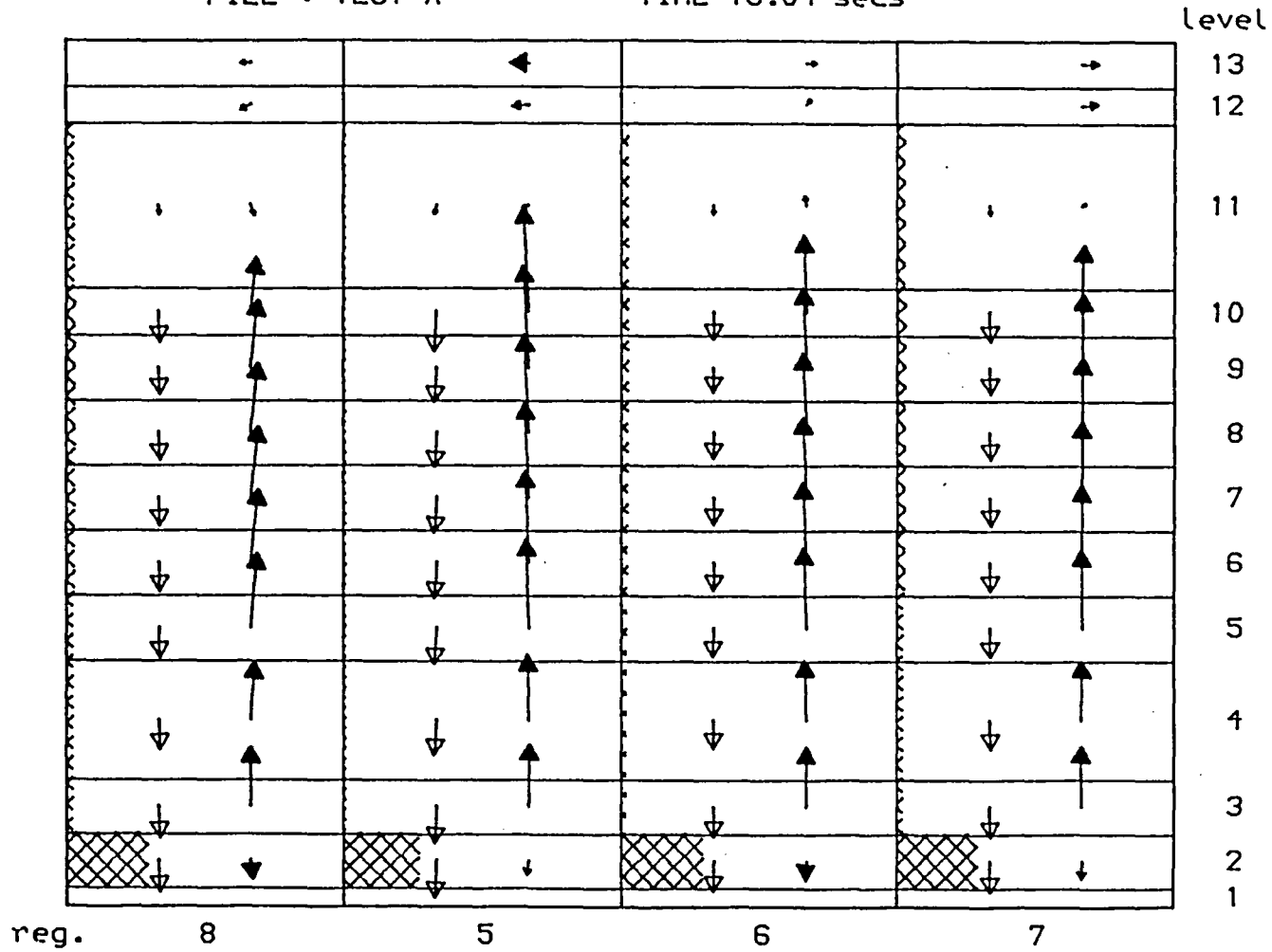


FIG. 5.3 TEST A ; VELOCITY VECTOR PLOT AND LIQUID FRACTION DISTRIBUTION IN DOWNCOMER

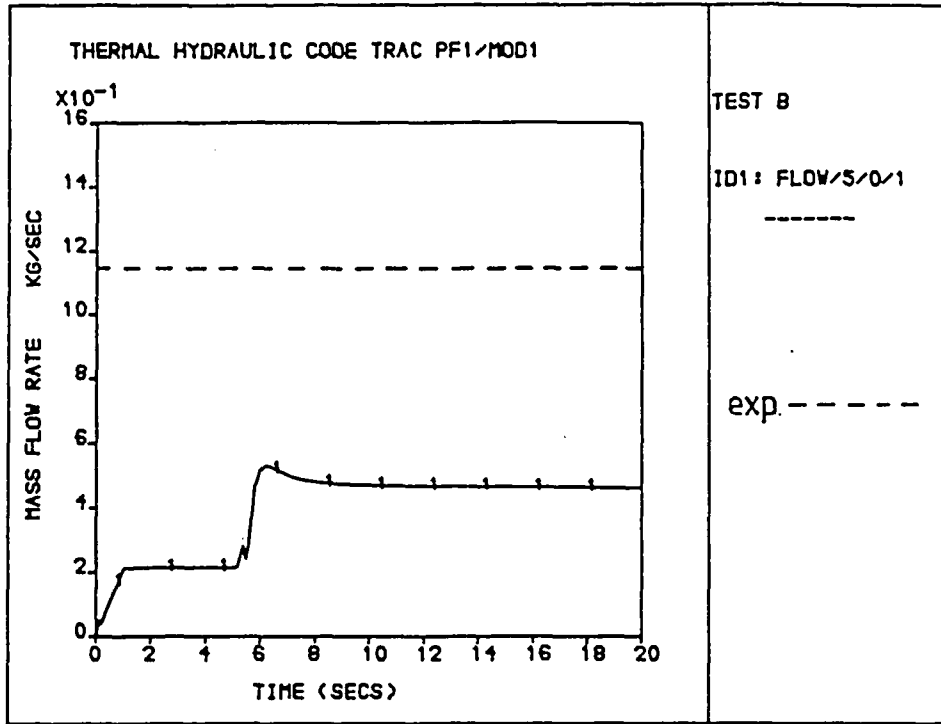


FIG. 5.4 TEST B ; EXPERIMENTAL AND PREDICTED BREAK MASS FLOWRATES

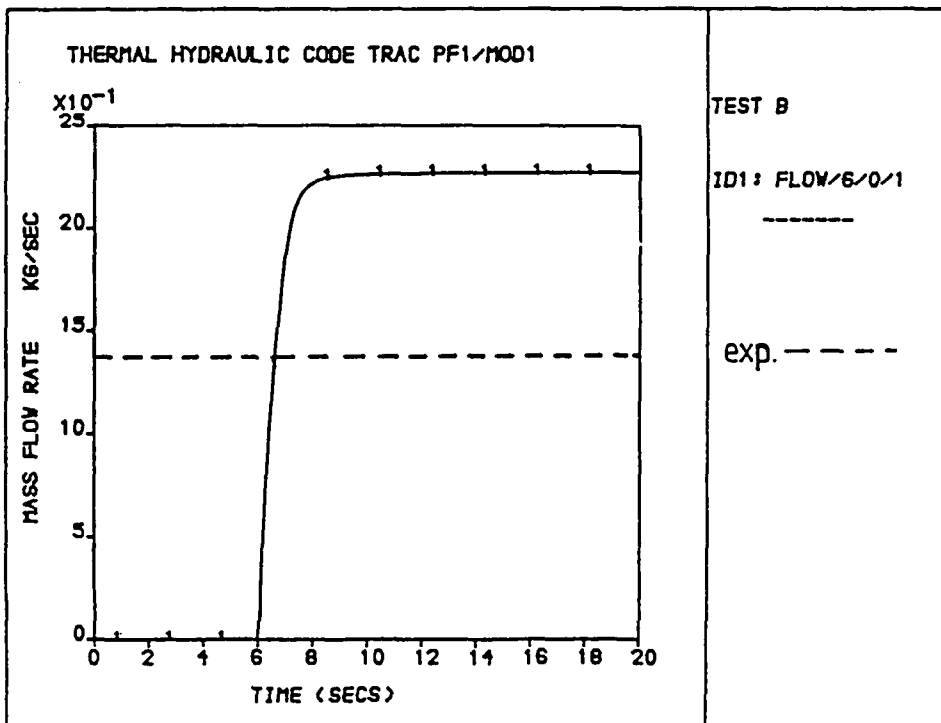


FIG. 5.5 TEST B ; EXPERIMENTAL AND PREDICTED MASS FLOWRATES FROM LOWER PLENUM

FILE : TEST B

TIME 19.03 secs

→ vap. vec.  
→ liq. vec.  
XXXX liq.frac.

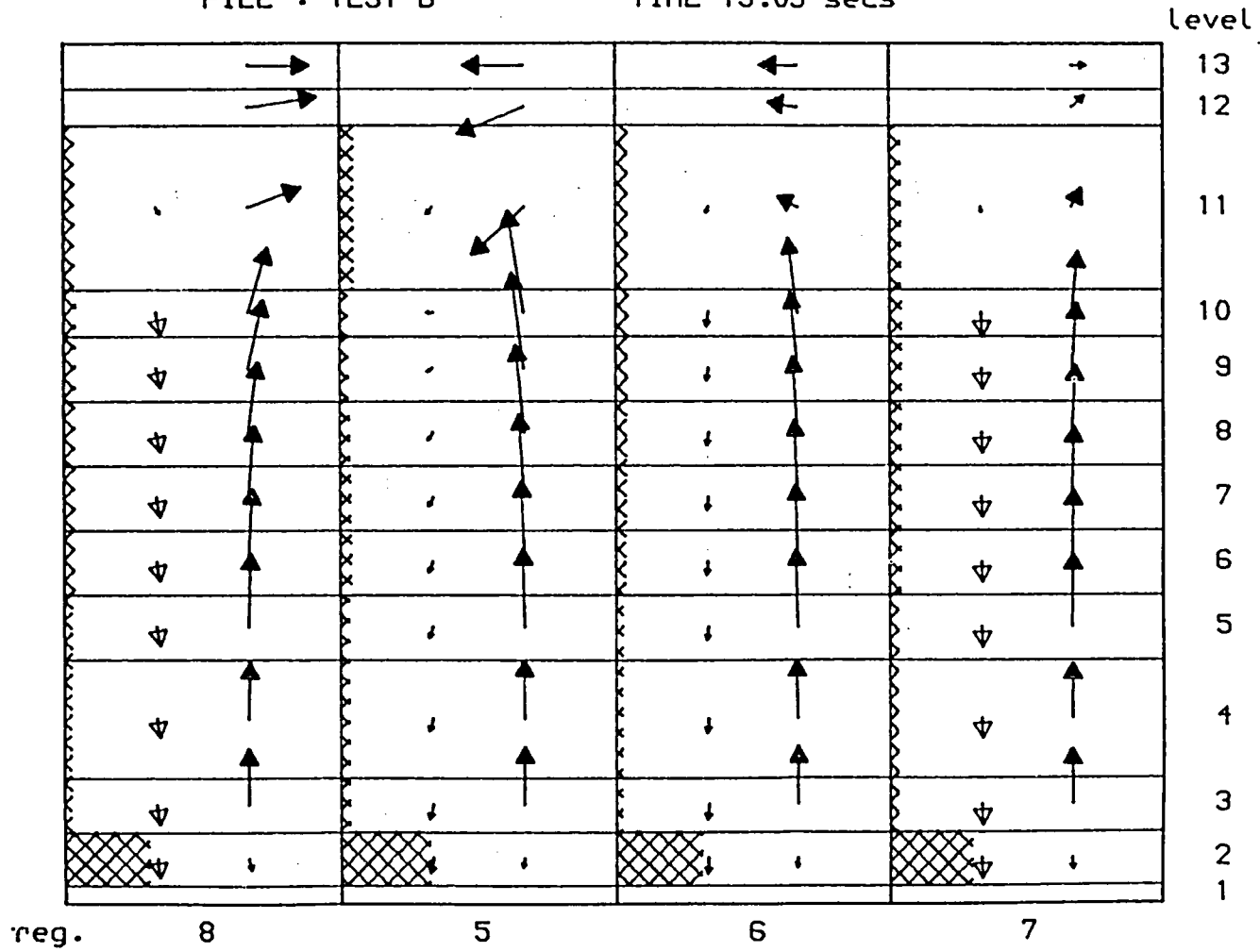


FIG. 5.6 TEST B ; VELOCITY VECTOR PLOT AND LIQUID FRACTION DISTRIBUTION IN DOWNCOMER

FILE : TEST B

TIME 19.03 secs

→ vap. vec.  
→ liq. vec.  
XXXXX liq. frac.

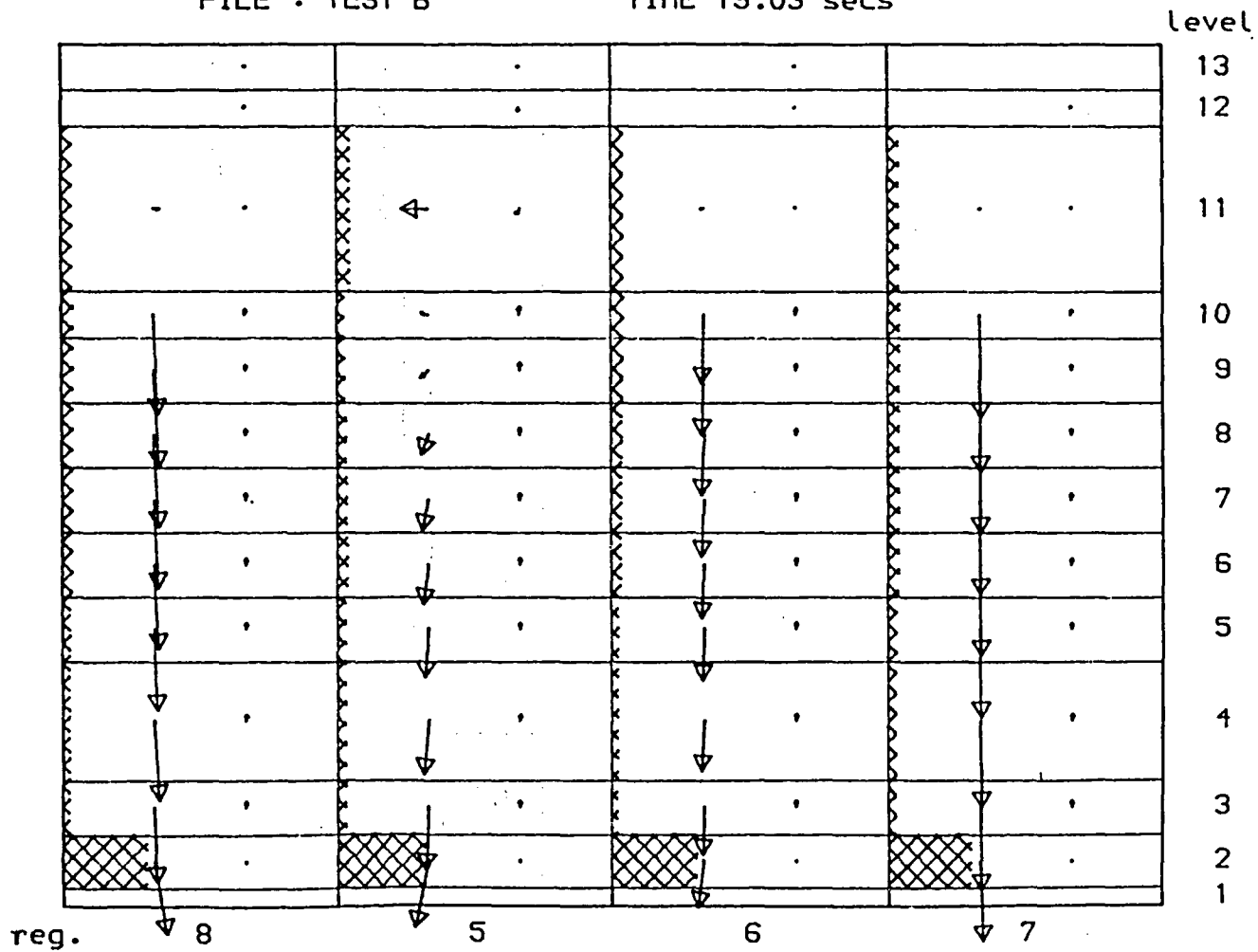


FIG. 5.7 TEST B : PHASIC MASSFLOW VECTORS AND LIQUID FRACTION DISTRIBUTION IN DOWNCOMER

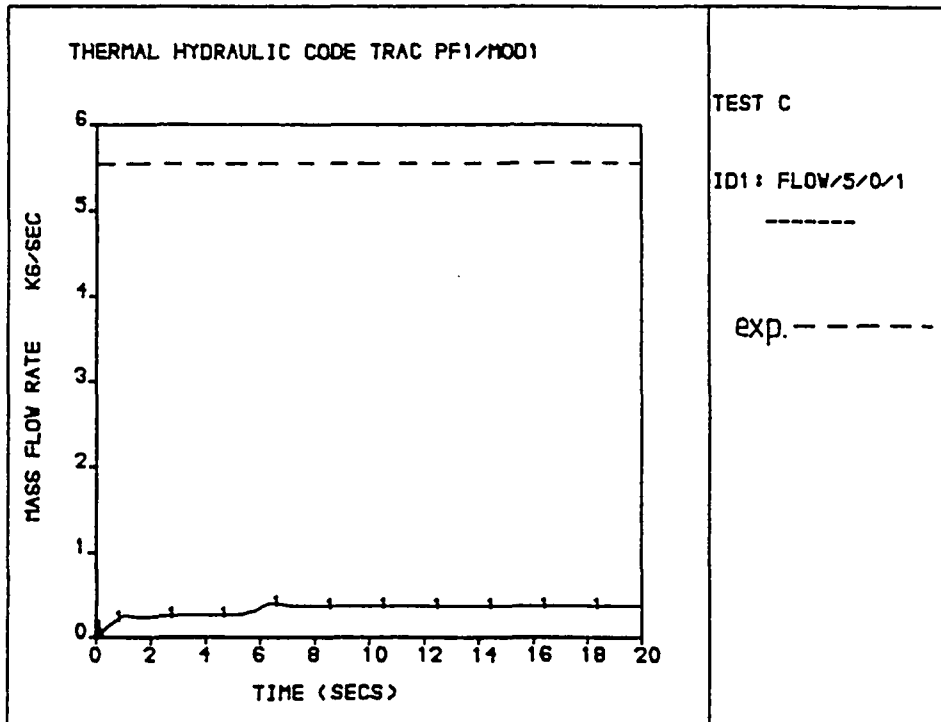


FIG. 5.8 TEST C ; EXPERIMENTAL AND PREDICTED BREAK MASS FLOWRATES

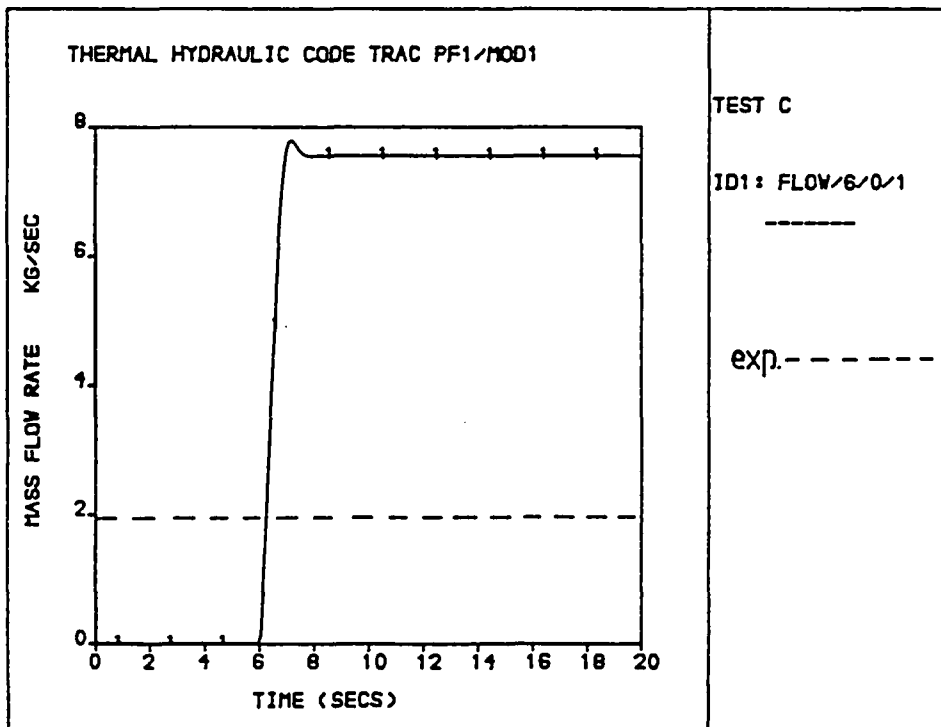


FIG. 5.9 TEST C ; EXPERIMENTAL AND PREDICTED MASS FLOWRATES FROM LOWER PLENUM

FILE : TEST C

TIME 19.06 secs

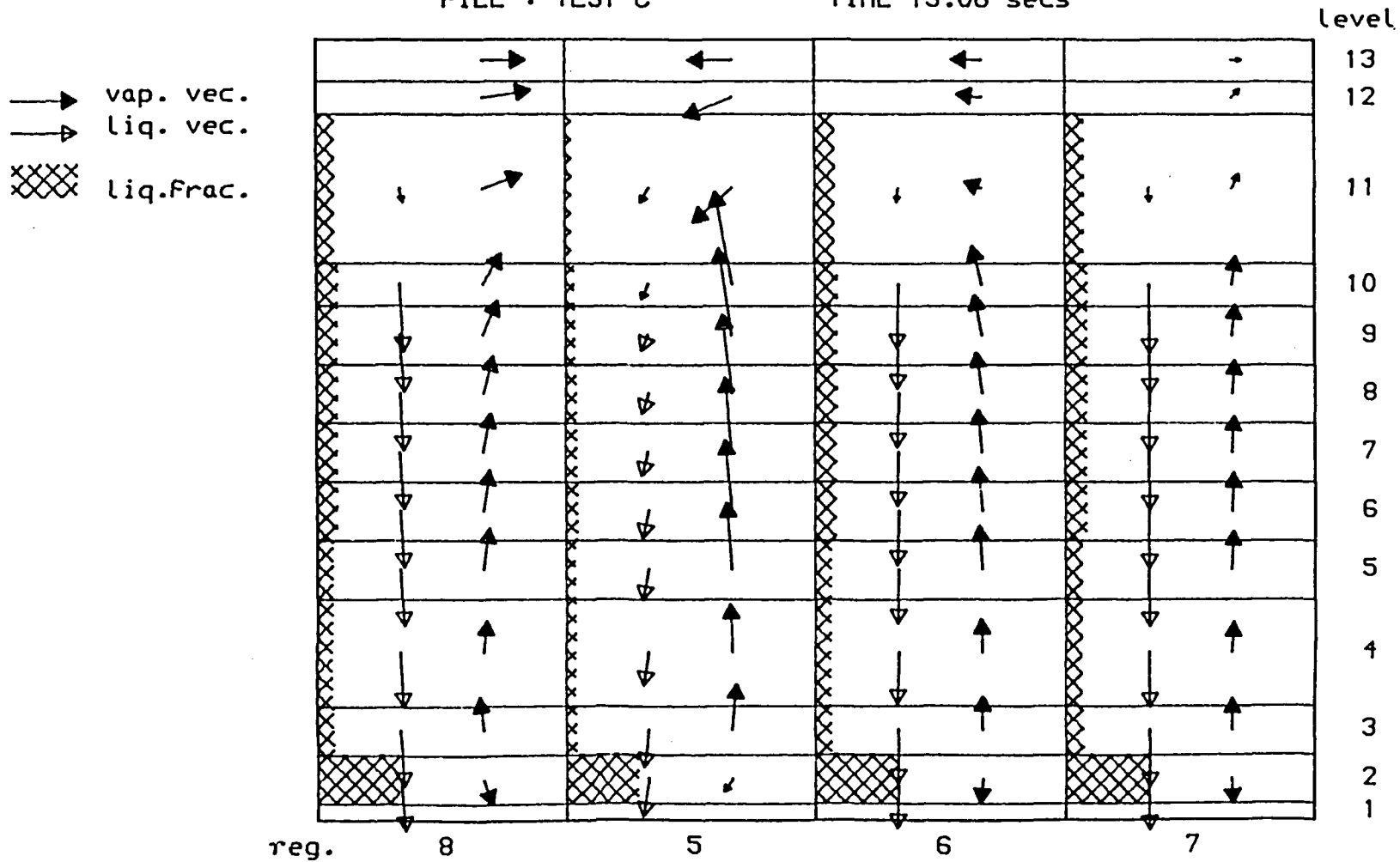


FIG. 5.10 TEST C ; VELOCITY VECTOR PLOT AND LIQUID FRACTION DISTRIBUTION IN DOWNCOMER

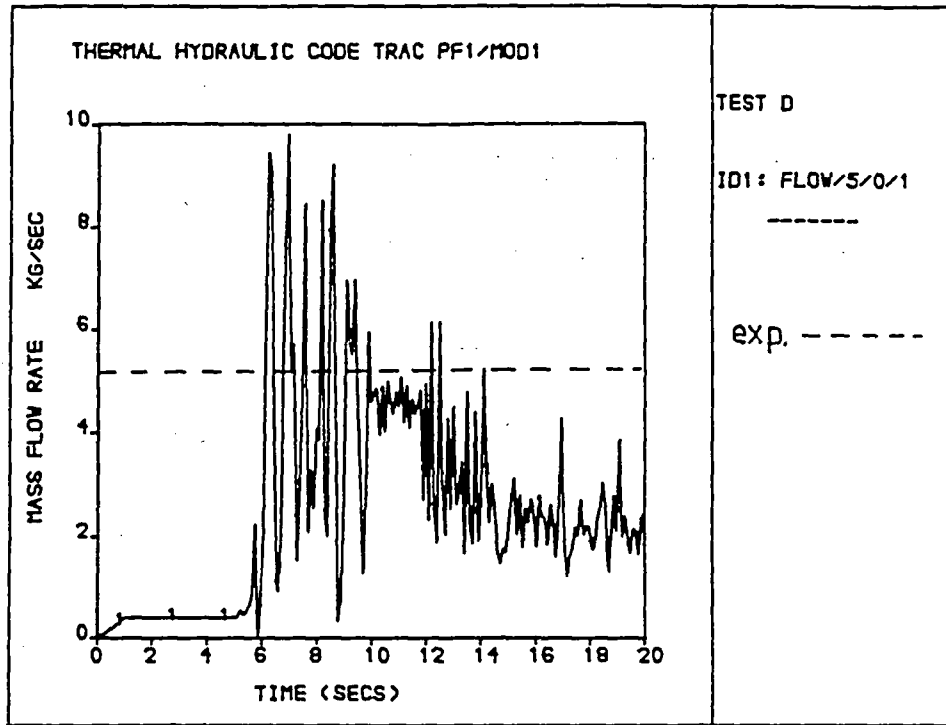


FIG. 5.11 TEST D ; EXPERIMENTAL AND PREDICTED BREAK MASS FLOWRATES

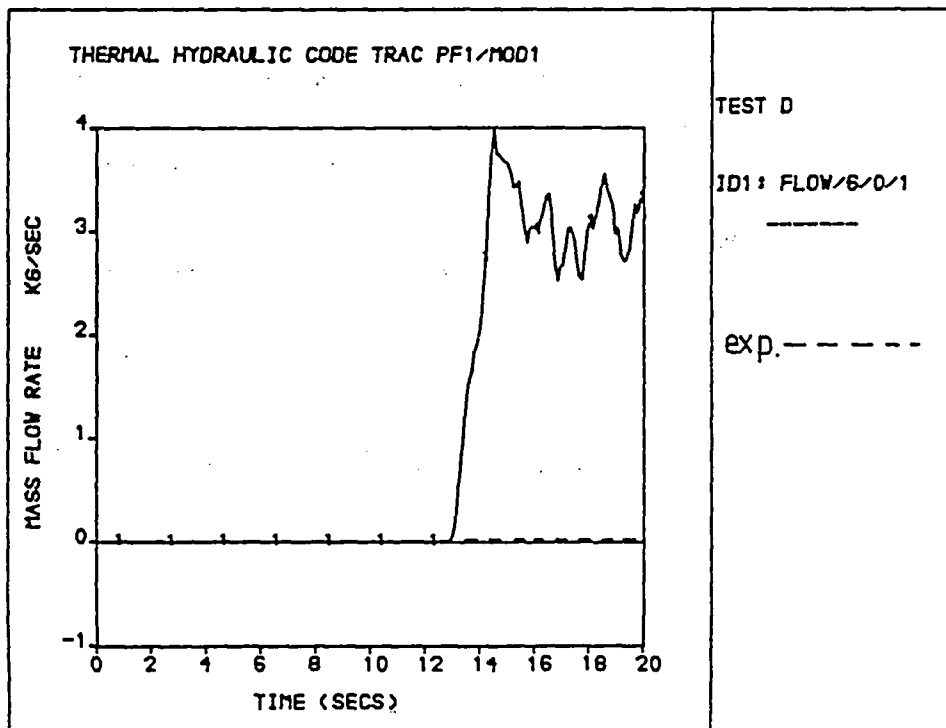


FIG. 5.12 TEST D ; EXPERIMENTAL AND PREDICTED MASS FLOWRATES FROM LOWER PLENUM

FILE : TEST D

TIME 19.56 secs

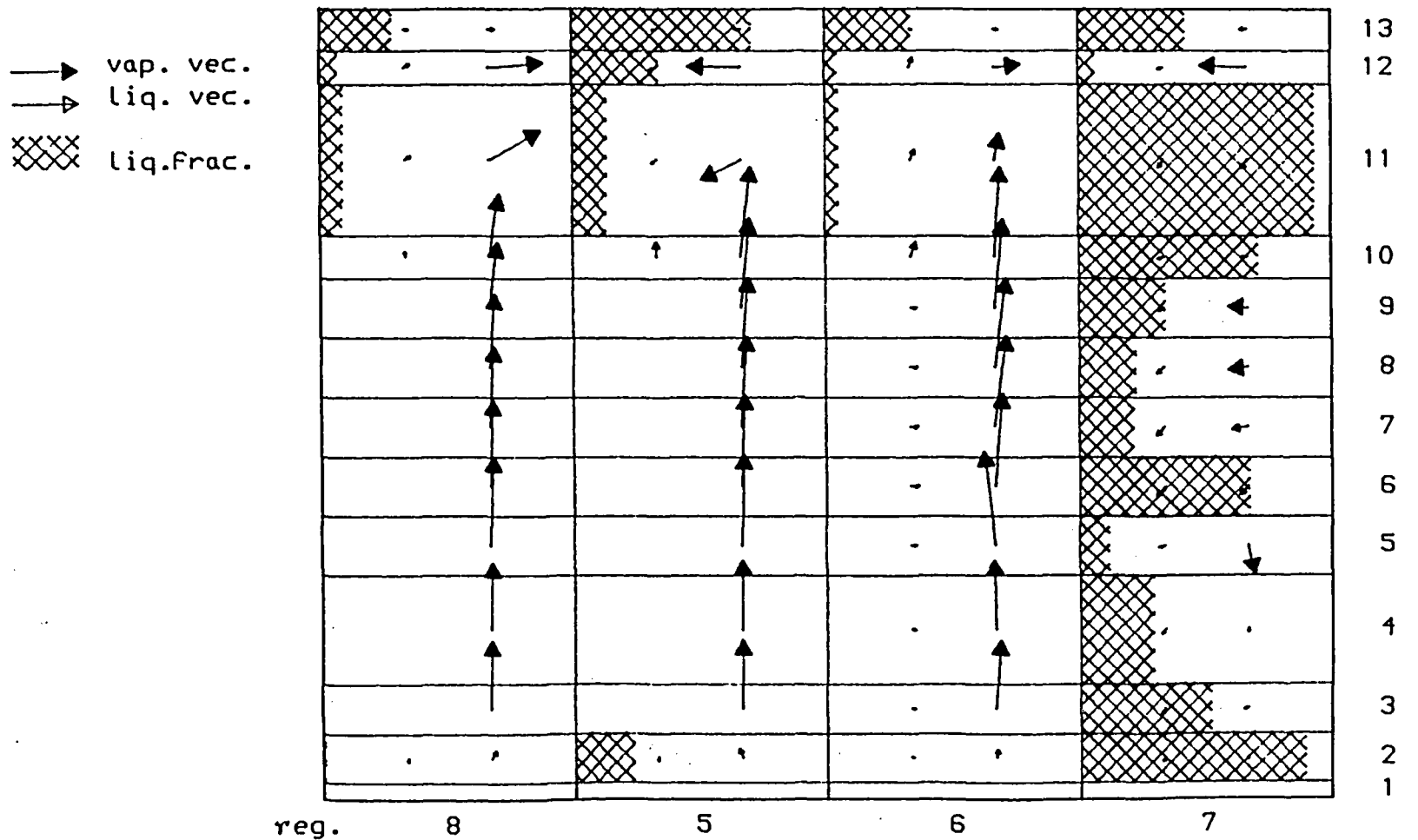


FIG. 5.13 TEST D ; VELOCITY VECTOR PLOT AND LIQUID FRACTION DISTRIBUTION IN DOWNCOMER

FILE : TEST D

TIME 19.56 secs

→ vap. vec.  
 → liq. vec.  
 XXXX liq.Frac.

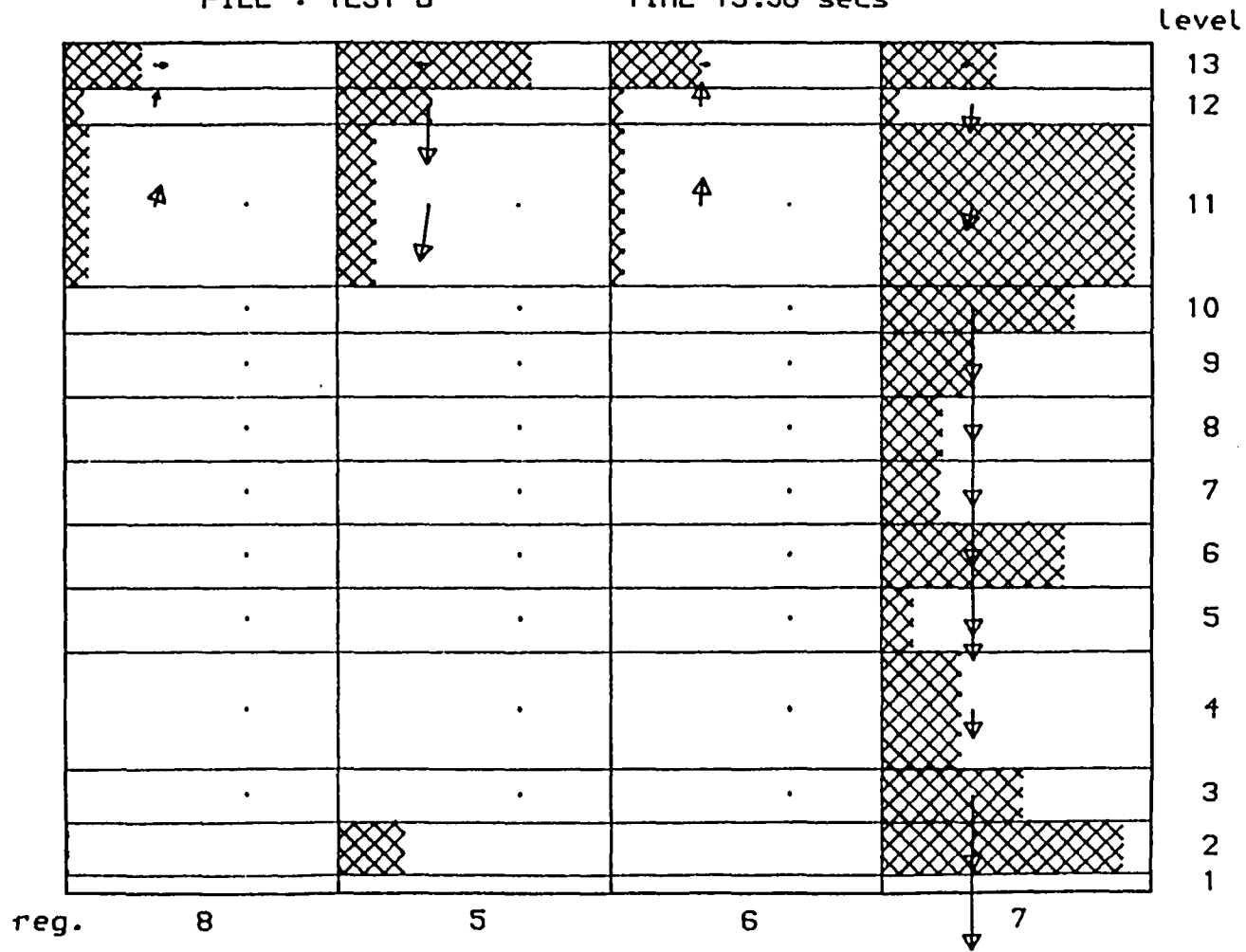


FIG. 5.14 TEST D ; PHASIC MASSFLOW VECTORS AND LIQUID FRACTION DISTRIBUTION IN DOWNCOMER

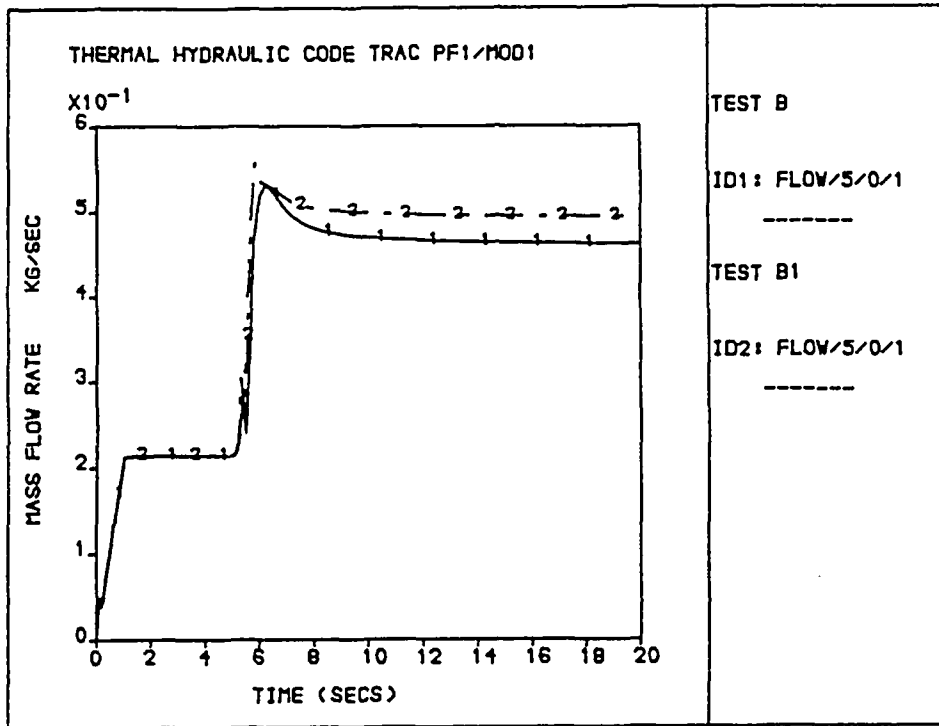


FIG. 5.15 COMPARISON OF STANDARD AND MODIFIED (TURNER) TRAC FOR TEST B-B1

FILE : TEST B1

TIME 19.04 secs

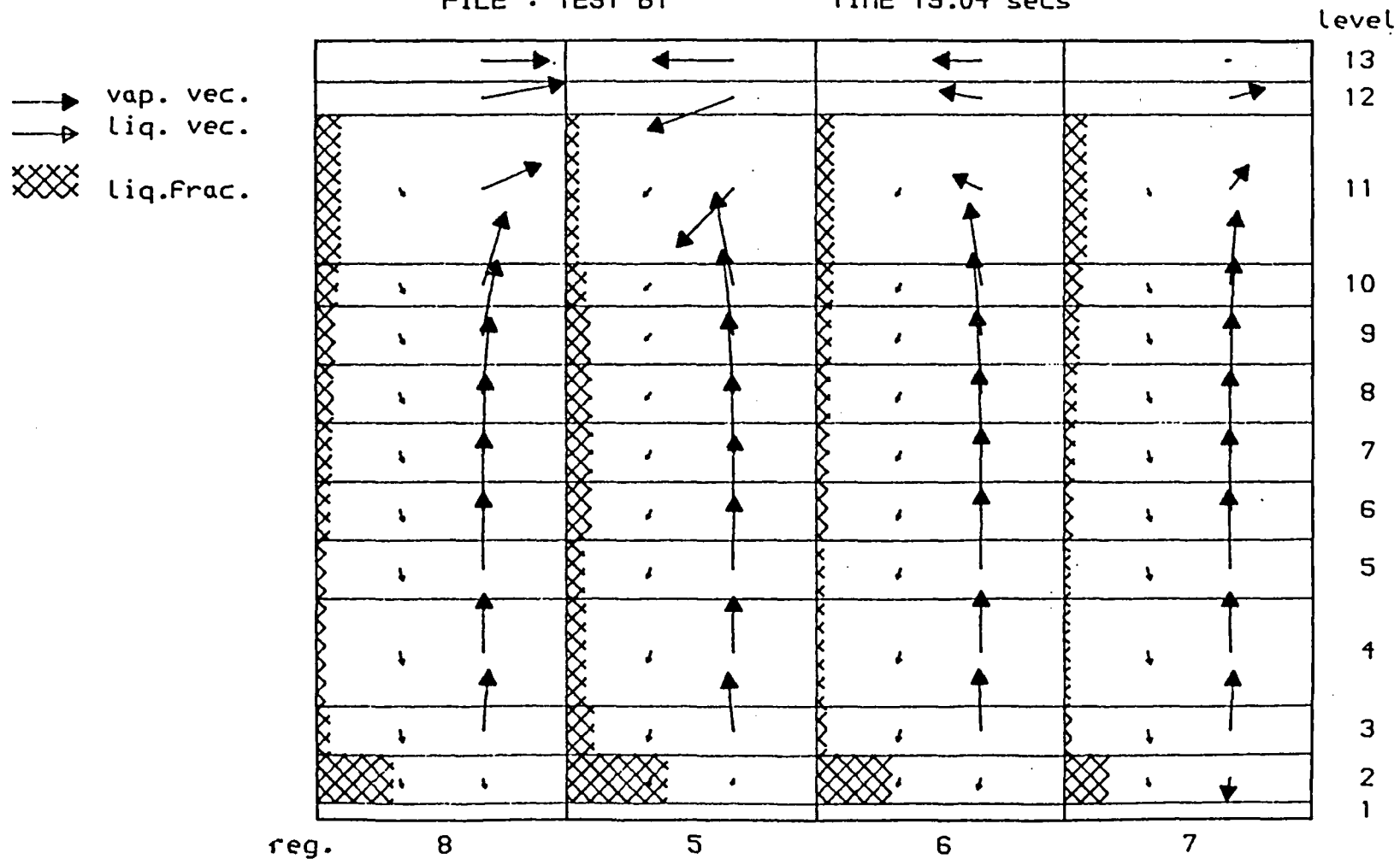


FIG. 5.16 TEST B1 : VELOCITY VECTOR PLOT AND LIQUID FRACTION DISTRIBUTION IN DOWNCOMER USING MODIFIED TRAC (TURNER)

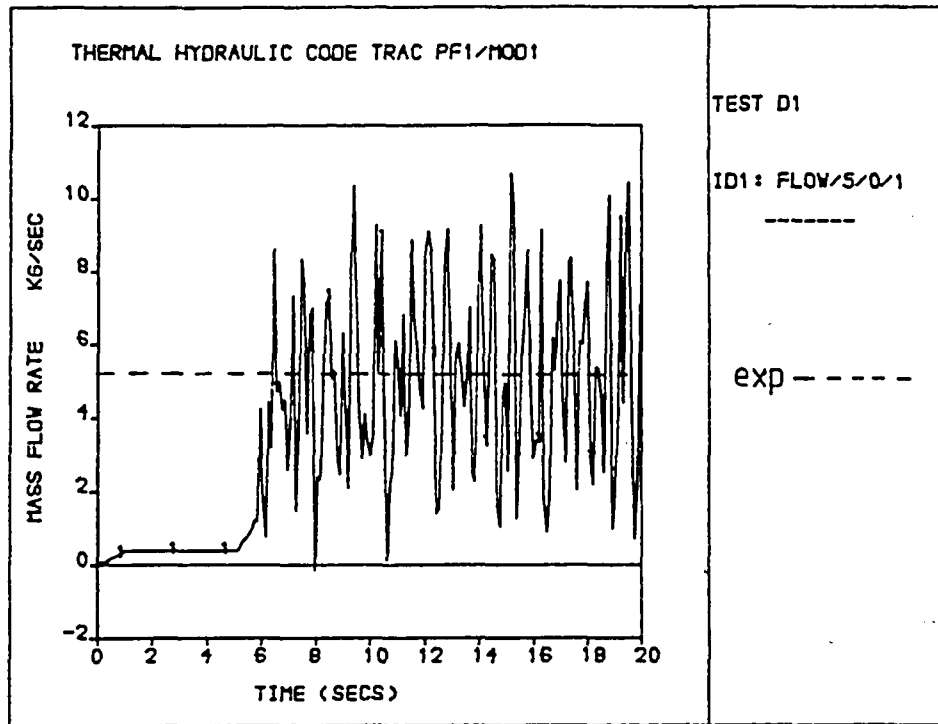


FIG. S.17 TEST D1 : EXPERIMENTAL AND PREDICTED BREAK MASS FLOWRATES USING MODIFIED TRAC (TURNER)

FILE : TEST D1

TIME 19.52 secs

→ vap. vec.  
→ liq. vec.  
XXXX liq.frac.

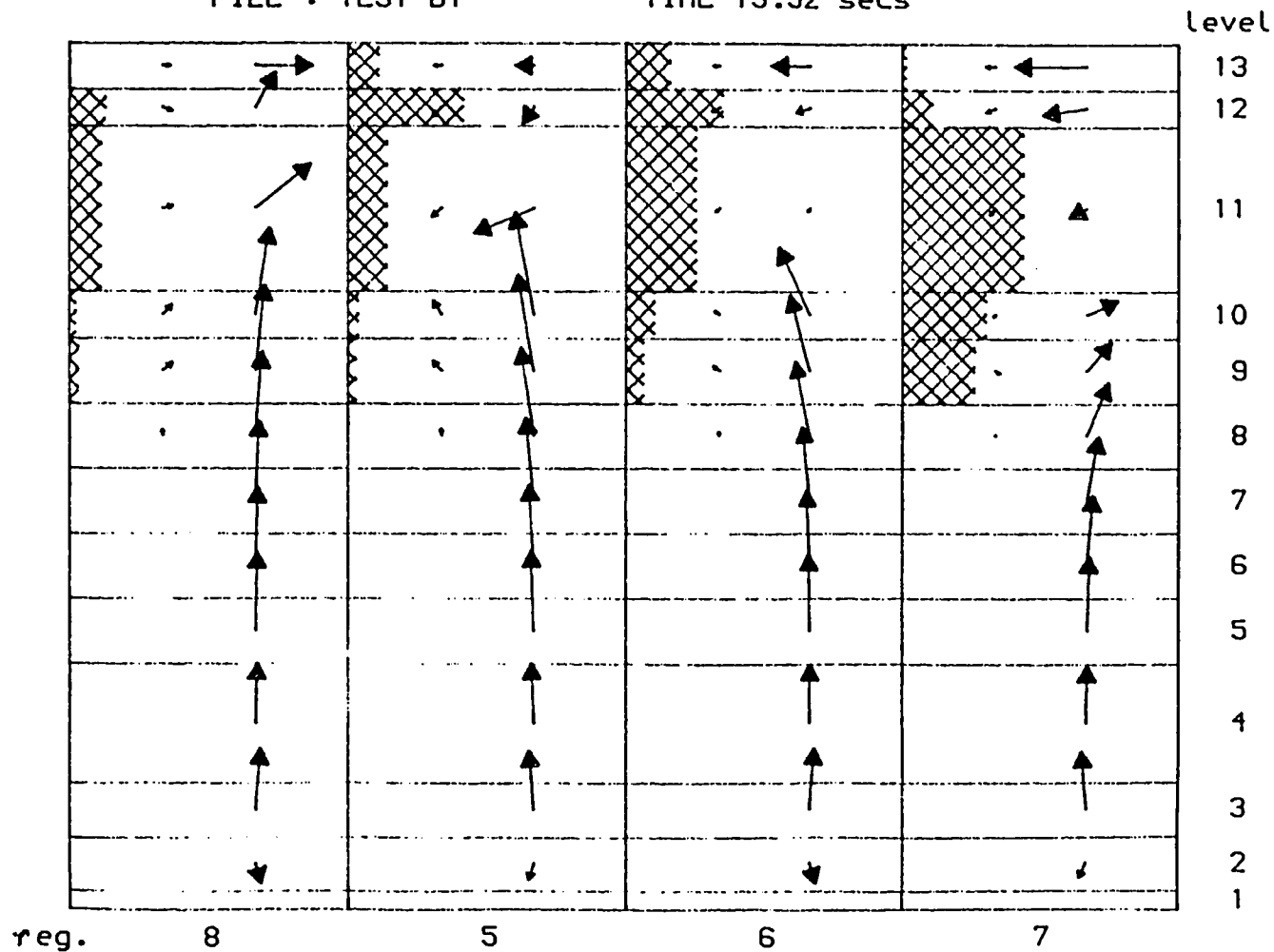


FIG. 5.10 TEST D1 : VELOCITY VECTOR PLOT AND LIQUID FRACTION DISTRIBUTION IN DOWNCOMER

FILE : TEST D1

TIME 19.52 secs

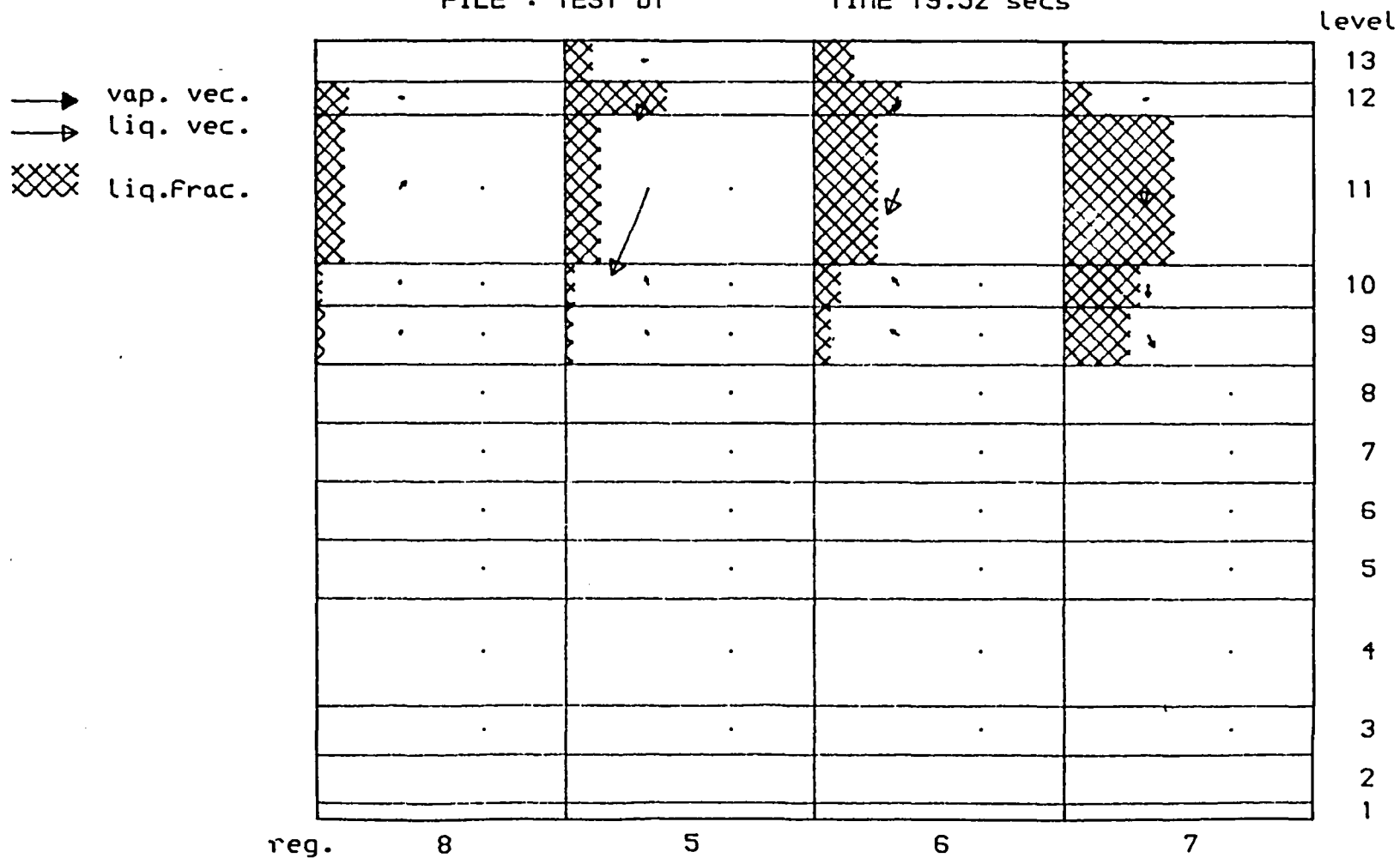


FIG. 5.19 TEST D1 ; PHASIC MASSFLOW VECTORS AND LIQUID FRACTION DISTRIBUTION IN DOWNCOMER

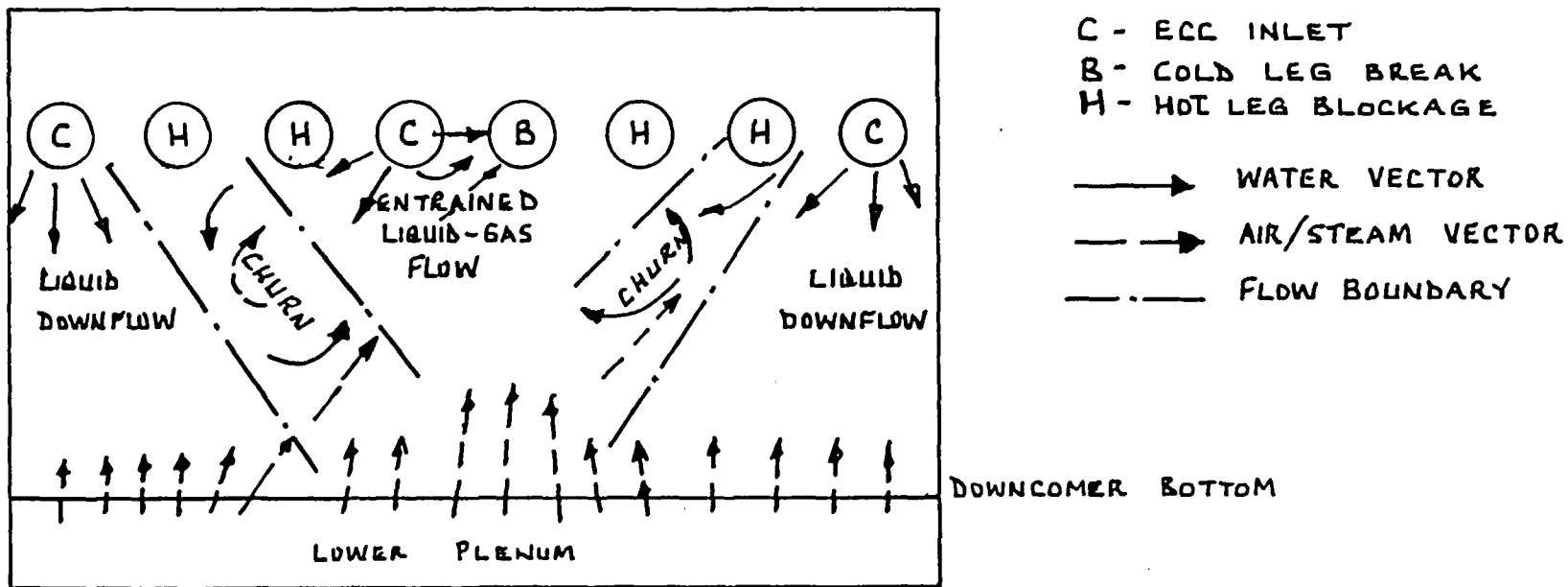


FIG. 6-1 SIMPLIFIED REPRESENTATION OF FLOW REGIMES IN ANNULAR DOWNCOMER DURING PARTIAL PENETRATION

$$Re_d = \frac{D_d V \rho_g}{\mu_g}$$

$Re_d < 0.1031$	$C_{D_d} = 240$
$0.1031 < Re_d < 989$	$C_{D_d} = \frac{24}{Re_d} (1 + 0.15 Re_d^{0.687})$
$Re_d > 989$	$C_{D_d} = 0.44$

Annular Mist Interfacial

Drag Coefficient,  $C_{iam} = C_{iaf}(1-E) + C_{im}(E)$  \_\_\_\_\_ (1)

where

$$C_{iaf} = \frac{0.01(1+75(1-\alpha)(1-E)\rho_g}{D_h}$$
 \_\_\_\_\_ (2)

and

$$C_{im} = \frac{\frac{3}{4} C_{D_d} (1-\alpha) \rho_g}{D_d}$$
 \_\_\_\_\_ (3)

$$D_d = \frac{\sigma We_d}{\rho_g V_r^2}$$

$$E = \text{Max.} \left( 7.75 \times 10^{-7} We^{1.25} Re_g^{0.25}, 1 - \exp\left(\frac{1}{2} \left(1 - \frac{V_g}{V_{olf}}\right)\right) \right)$$
 \_\_\_\_\_ (4)

with

$$We = \frac{\rho_g j_g^2 D_h}{\sigma} \left(\frac{\Delta \rho}{\rho_g}\right)^{\frac{1}{3}}$$

$$Re_g = \frac{\rho_g j_g D_h}{\mu_g}$$

$$V_{olf} = 2.33 \left(\frac{\Delta \rho \cdot \sigma We_d}{N \rho_g}\right)^{\frac{1}{4}}$$

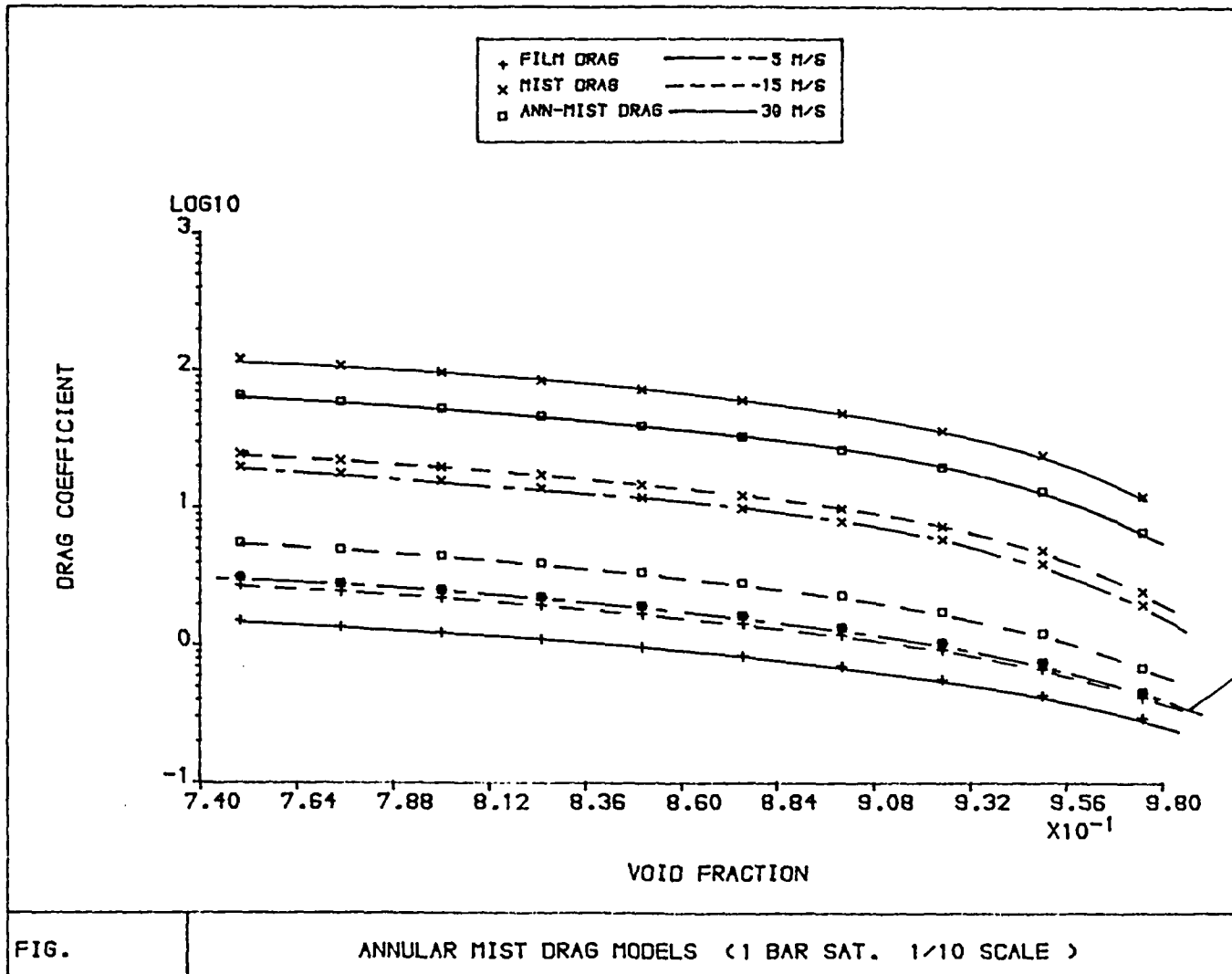


FIG. 7.2 COMPARISON OF TRAC ANNULAR MIST DRAG COEFFICIENTS FOR VARIOUS VAPOUR VELOCITIES AND VOID FRACTIONS

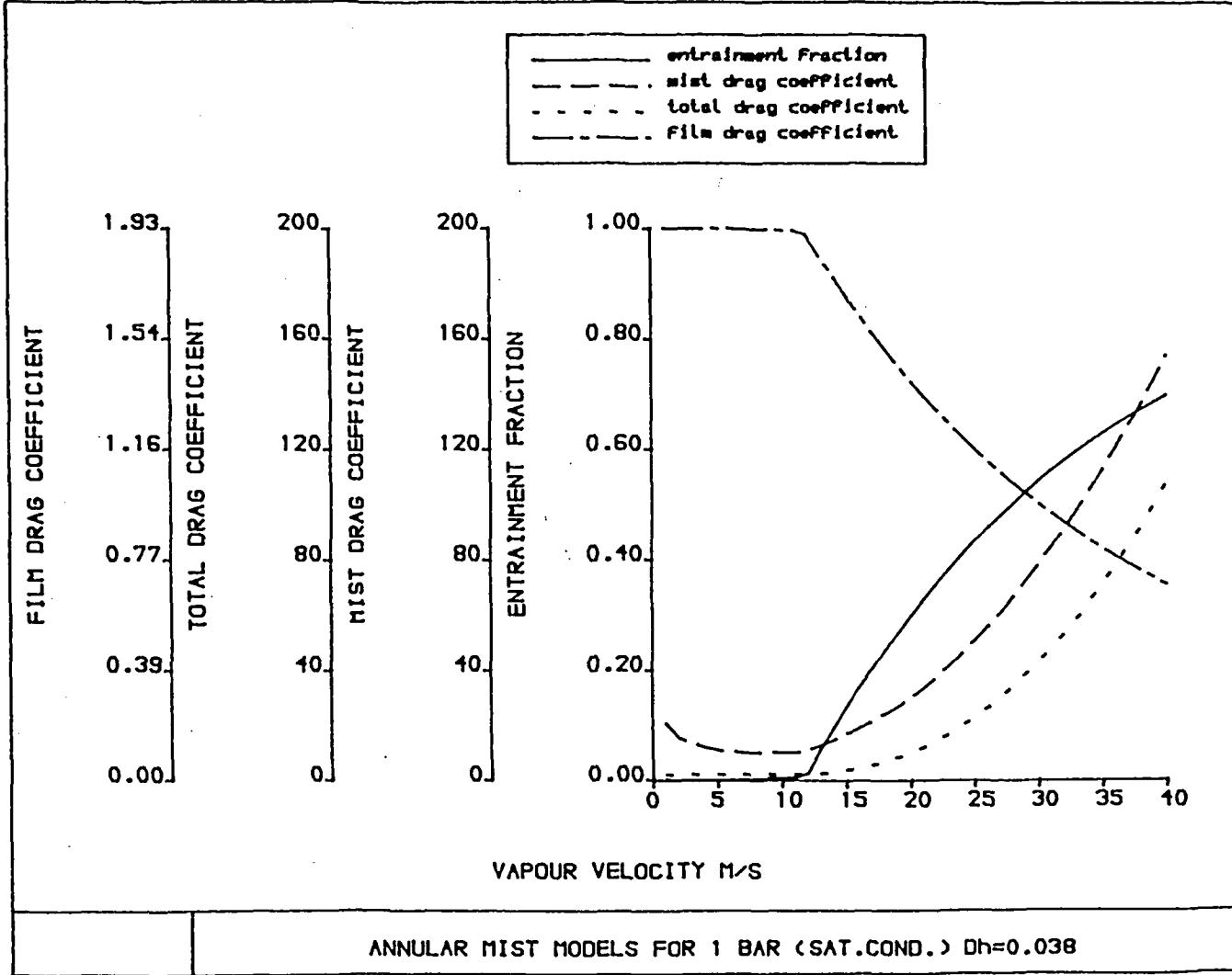


FIG. 7.3 ENTRAINMENT FRACTION, MIST, FILM AND TOTAL DRAG COEFFICIENTS WITH VARIATION IN VAPOUR VELOCITIES FOR 1/10 SCALE MODEL CONDITIONS

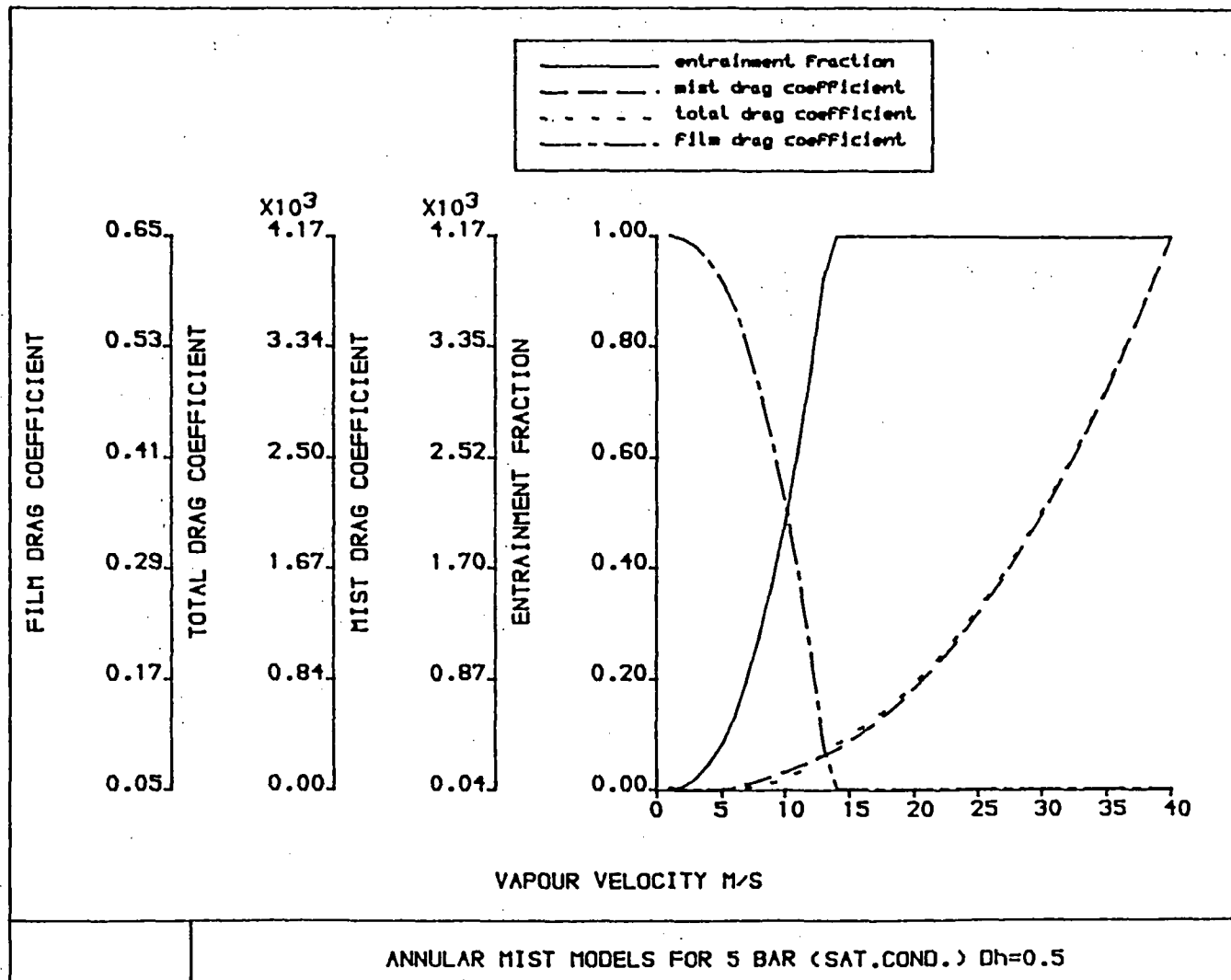


FIG. 7.4 ENTRAINMENT FRACTION, MIST, FILM AND TOTAL DRAG COEFFICIENTS WITH VARIATION IN VAPOUR VELOCITIES FOR FULL SCALE CONDITIONS

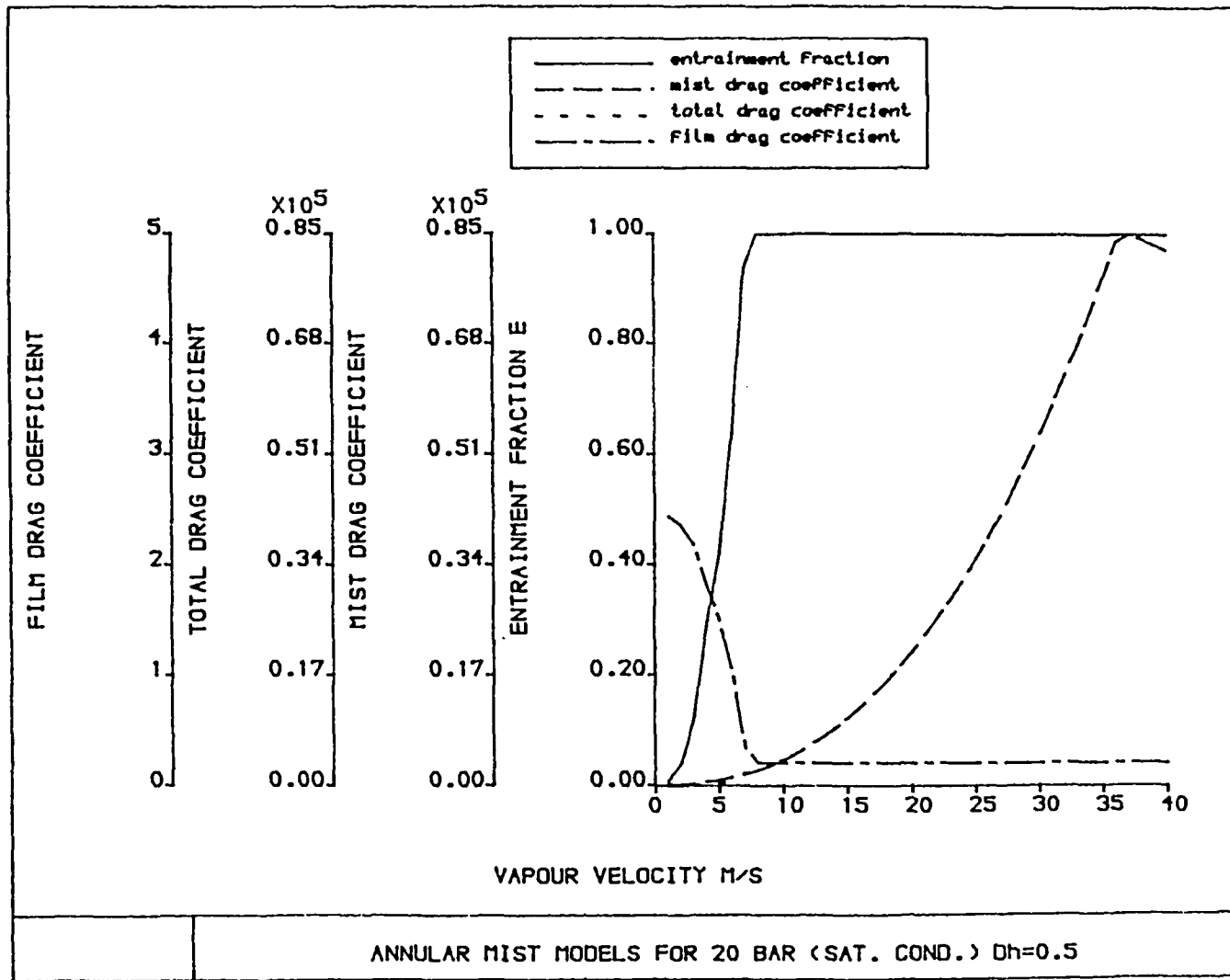


FIG. 7.5 ENTRAINMENT FRACTION, MIST, FILM AND TOTAL DRAG COEFFICIENTS WITH VARIATION IN VAPOUR VELOCITIES FOR FULL SCALE CONDITIONS



**BIBLIOGRAPHIC DATA SHEET**

*(See instructions on the reverse)*

1. REPORT NUMBER  
(Assigned by NRC, Add Vol., Supp., Rev.,  
and Addendum Numbers, if any.)

NUREG/IA-0055

2. TITLE AND SUBTITLE

An Assessment of TRAC-PF1/MOD1 Using Strathclyde 1/10 Scale  
Model Refill Tests

3. DATE REPORT PUBLISHED

MONTH	YEAR
March	1992

4. FIN OR GRANT NUMBER

A4682

5. AUTHOR(S)

W.M. Dempster, A.M. Bradford, T.M.S. Callander, H.C. Simpson

6. TYPE OF REPORT

Technical

7. PERIOD COVERED *(Inclusive Dates)*

8. PERFORMING ORGANIZATION - NAME AND ADDRESS *(If NRC, provide Division, Office or Region, U.S. Nuclear Regulatory Commission, and mailing address; if contractor, provide name and mailing address.)*

University of Strathclyde/Central Electricity Research Laboratories  
Kelvin Avenue  
Leatherhead, Surrey  
United Kingdom

9. SPONSORING ORGANIZATION - NAME AND ADDRESS *(If NRC, type "Same as above"; if contractor, provide NRC Division, Office or Region, U.S. Nuclear Regulatory Commission, and mailing address.)*

Office of Nuclear Regulatory Research  
U.S. Nuclear Regulatory Commission  
Washington, DC 20555

10. SUPPLEMENTARY NOTES

11. ABSTRACT *(200 words or less)*

TRAC-PF1/MOD1 predictions of LOCA Refill Experiments carried out on a 1/10 scale model PWR vessel are presented. The predictions show that TRAC underpredicts bypass for the test cases considered. Comparison results are presented and discussed. Simple sensitivity analysis of the interfacial drag models used is presented in an effort to explain the performance of the code.

12. KEY WORDS/DESCRIPTORS *(List words or phrases that will assist researchers in locating the report.)*

ICAP Program, TRAC-PF1/MOD1, LOCA Refill

13. AVAILABILITY STATEMENT

Unlimited

14. SECURITY CLASSIFICATION

*(This Page)*

Unclassified

*(This Report)*

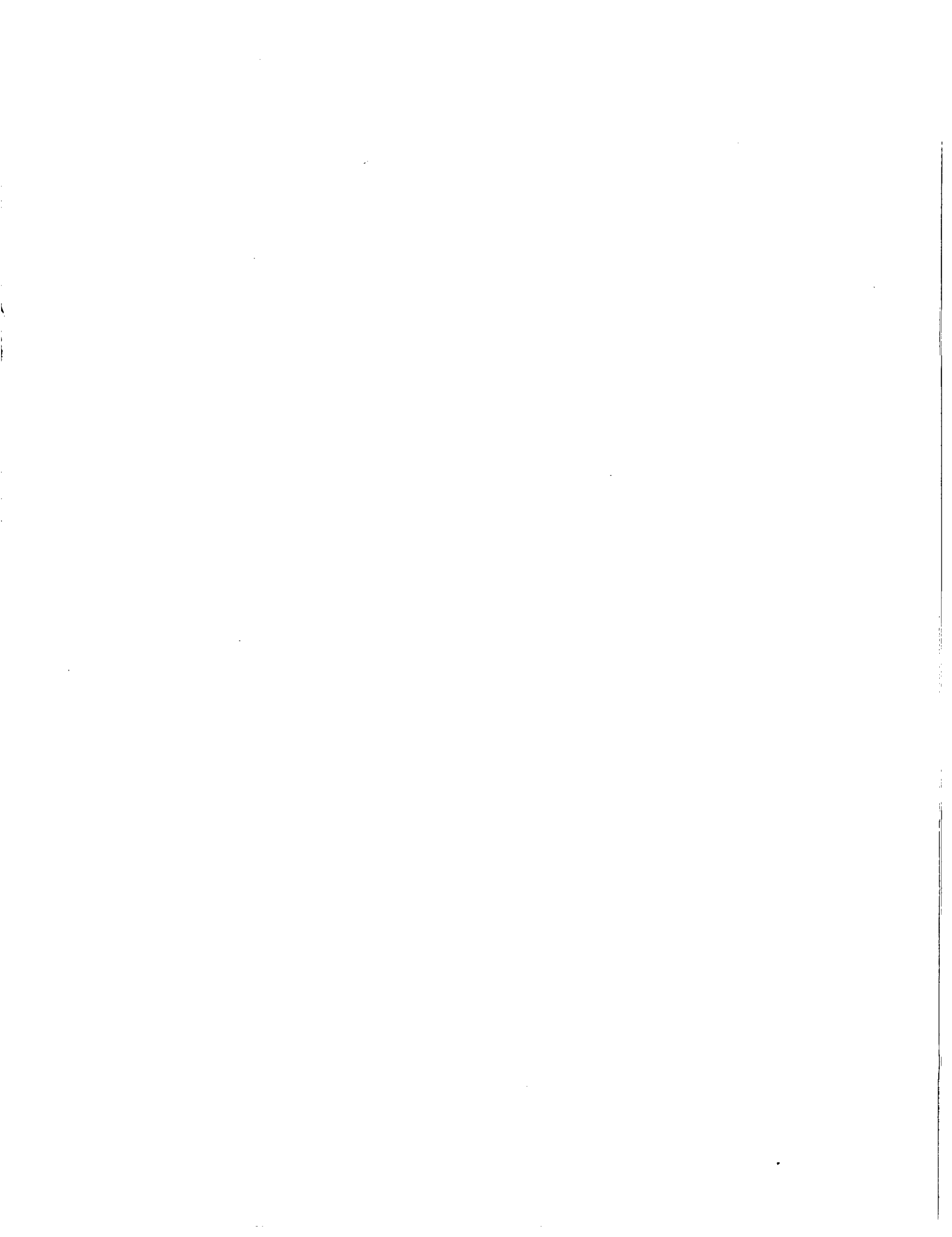
Unclassified

15. NUMBER OF PAGES

16. PRICE



**THIS DOCUMENT WAS PRINTED USING RECYCLED PAPER**



UNITED STATES  
NUCLEAR REGULATORY COMMISSION  
WASHINGTON, D.C. 20555

OFFICIAL BUSINESS  
PENALTY FOR PRIVATE USE, \$300

SPECIAL FOURTH-CLASS RATE  
POSTAGE & FEES PAID  
USNRC  
PERMIT No. G-67

NUREG/IA-0055

AN ASSESSMENT OF TRAC-PFI/MOD1 USING STRATHCLYDE 1/10 SCALE MODEL REFILL TESTS

MARCH 1992